Exploring CDC20 gene expression in oral cavity cancer

Dissertação apresentada no Instituto Superior Ciências da Saúde – Norte, para obtenção do grau de Mestre em Terapias Moleculares

Orientador: Doutor Hassan Bousbaa

Co-orientador: Doutor Luís Monteiro

Instituto Superior de Ciências de Saúde – Norte

CICS - Centro de Investigação em Ciências da Saúde

Grupo de Biologia Molecular e Celular

ISCSN/CESPU, Rua Central de Gandra, 131, 4585-116 Gandra PRD

Portugal

Acknowledgements

Gostaria de agradecer ao Professor Doutor Hassan Bousbaa, meu orientador, pela sua disponibilidade e conhecimentos transmitidos, pela enorme boa disposição, pelas oportunidades e votos de confiança depositados em mim e ainda pelo seu profissionalismo que foi sempre uma forte motivação fazendo-me querer ir mais longe.

Ao Professor Doutor Luís Monteiro pela disponibilidade, conhecimentos transmitios e pelo apoio incondicional durante o desenvolvimento do meu trabalho.

Às minhas amigas, Kamonporn Masawang, Kelly Ascenção, Joana Barbosa, Juliana Faria, Patrícia Silva, Rita Reis e Vanessa Nascimento pela disponibilidade, paciência, amizade, amabilidade e por todo o apoio tendo-me dado coragem e segurança no desenvolvimento do meu trabalho no laboratório.

À Professora Doutora Roxana Falcão e Professora Doutora Odília Queirós pelo profissionalismo, incentivo e pela confiança depositada em mim ao longo do meu percurso universitário.

Ao Instituto e ao CICS pela oportunidade de integração neste projecto.

Aos meus amigos de turma, Andrea Cunha, Diana Valente, Francisca Araújo, João Barbosa, Jorge Mota, Miguel Azevedo e Rita Malheiro por me acompanharem ao longo do mestrado sempre com muito apoio, carinho e atenção.

À minha família, pelas pessoas maravilhosas que são, pela confiança que sempre depositaram em mim, pelas palavras de apoio e pelo esforço todo que fizeram e continuam a fazer por mim para que possa ter um futuro melhor.

Aos meus queridos amigos Ana Curinha, João Oliveira, Marta Andorinha, Rita Taveira e Sara Vaz por tudo o que me proporcionaram ao longo destes anos, todo o apoio e coragem, assim como todas as gargalhadas e todos os bons momentos. Ao Ricardo Blanquett pela pessoa fantástica que é, pela força e palavras de incentivo e pelo constante carinho e boa disposição. Todos eles, são parte essencial do meu mundo.

This work was supported by grant (01-GCD-CICS-09; 02-GCD-CICS-09; and 05-GCD-CICS-2011) from Cooperativa de Ensino Superior Politécnico e Universitário (CESPU).

The results presented in this dissertation are part of the following publications and scientific communications:

Book chapter

Faria J, Barbosa J, **Moura I**, Reis RM, Bousbaa H (2011). The Spindle Assembly Checkpoint and Aneuploidy. In Aneuploidy: Etiology, Disorders and Risk Factors. ISBN: 978-1-62100-070-9. Nova Science Publishers, Inc.

Original article

Inês MB Moura, Maria L. Delgado1, Patrícia MA Silva, C arlos A Lopes, José B do Amaral, Luís S Monteiro, Hassan Bousbaa. High C DC 20 expression is associated with poor prognosis in oral squamous cell carcinoma. J Oral Pathol Med (in press)

Poster

Inês M. B. Moura, Maria L. Delgado, Patrícia M. A. Silva, C arlos A. Lopes, José B. do Amaral, Luís S. Monteiro, Hassan Bousbaa (2013). High CDC20 expression is associated with poor prognosis in oral squamous cell carcinoma. XXII Porto Cancer Meeting & III Porto-Bordeaux Joint Meeting, April 2013, IPATIMUP, Porto Portugal.

Oral communication

Inês M. B. Moura. Resource work presentation: "Interfering with mitotic checkpoint gene expression in tumor cells" – CIBEME (Congresso ibérico de estudantes de medicina), 27 October 2010, University of Santiago de Compostela, Spain.

Inês M. B. Moura. Resource work presentation: "Exploring CDC20 gene expression in oral cavity cancer" – IX Ciclo de Conferências, CESPU, 18 April 2013, EXPONOR, Porto Portugal.

Index

Image Index ..... **VI**

Table Index ..... **VIII**

Abstract ..... **IX**

Resumo ..... **X**

Abbreviations ..... **XI**

Introdução **1**

1. **The cell cycle** 2
2. **Mitosis** 3
3. **Cell cycle regulation** 6
4. **The spindle assembly checkpoint** 7
   - 4.1 **Molecular pathway of the SAC** 8
   - 4.2 **SAC defects in cancer** 11
5. **Targeting the SAC as a cancer therapy strategy** 13
6. **SAC components as cancer biomarkers** 14
7. **The oral cavity cancer and SAC** 15
8. **CDC20 expression in OSCC** 16

Aim of the study **17**

Material and Methods **18**

Tissue microarray (TMA) construction 19

Immunohistochemistry 19

Evaluation of immunohistochemistry 19

Microscopy, image acquisition and processing 20

Statistical analysis 20

Cell culture 20

Cell freezing and thawing 21

Coating of glass coverslips with poly-L-lysine 21

RNA Interference 21

Cytospin 22

Immunofluorescence 22

Protein extraction and quantification 23

Western blotting 23

Microscopy, image acquisition and processing 24

Results and discussion **24**

1. CDC20 as a potential biomarker for OSCC 26

1.1 Evaluation of CDC20 expression in human OSCC tissues 26

1.2 CDC20 expression and its correlation to clinicopathological parameters in OSCC 28

1.3 CDC20 expression and prognostic significance in OSCC 30

2. CDC20 as a potential therapeutic target 37

2.1 Evaluation of CDC20 protein depletion efficiency 37

2.2 Analysis of the phenotype resulting from CDC20 depletion 40

Conclusion **45**

Future prospects **47**

References **49**

Image Index

Figure 1: Kinetochore-microtubule interactions. A: during prometaphase, one sister chromatid is attached to microtubule from only on spindle pole (monotelic attachment) and a wait signal is generated. B: at metaphase, both sister chromatid become attached to microtubules from both spindle pole (amphitelic attachment) with the appropriate tension [19]..... 4

Figure 2: Representation of cell cycle phases. Interphase comprises G1, S and G2 phases. In G1 and G2 the cell grows and RNA and proteins are synthesized. At S phase the DNA and centrosomes are replicated. At the end of prophase the chromosomes must be condensed and the matured centrosomes must move towards the opposite poles. During the prometaphase the kinetochores must be captured by microtubules from mitotic spindle. At metaphase the chromosomes must be properly aligned at metaphase plate to allow sister-chromatid separation in anaphase. In telophase nucleus division occurs and is followed by two daughter cells' formation in cytokinesis [12]..... 5

Figure 3: Cell cycle regulation by cyclin-dependent protein kinases (Cdks). Schematic representation of cdks involved in progression of the cell cycle. The cyclin D-Cdk4/6 complex controls the cell cycle entry, the cyclin E-Cdk2 complex promotes the initiation of DNA replication, the cyclin A-Cdk2 complex stimulates DNA replication and lastly, the cyclin B-cdk1 complex is essential for entry and development of mitosis (Adapted from [26])..... 7

Figure 4: Molecular pathway of spindle assembly checkpoint (SAC). A: The presence of unattached or improperly attached chromosomes leads to SAC activation. An inhibitory signal is generated by the mitotic checkpoint complex (MCC) comprised by BubR1, Bub3 and Mad2. CDC20 is sequestered and the APC/C remains inactive preventing securin and cyclin B degradation and the cycle is arrested. B: When all chromosomes are properly aligned in metaphase plate the SAC is silenced. CDC20 is free to bind and activate the APC/C that targets securin and cyclin B to proteolysis. Securin degradation leads to separase activation and sister-chromatid separation. Cyclin B degradation results in mitotic exit [40]..... 10

Figure 5: A defective SAC can lead to aneuploidy. In normal cells with a competent SAC, the chromosome missegregation is prevented. In cell with a defective SAC, the

residual checkpoint activity is sufficient to ensure the accuracy of chromosome segregation [40]. 12

Figure 6: CDC20 protein expression in oral squamous cell carcinoma (OSCC). CDC20 was detected by immunohistochemistry using monoclonal mouse anti-CDC20 antibody; counterstaining was performed with haematoxylin. A: CDC20 staining in epithelial cells in normal oral mucosa, x400. B D: Low levels of CDC20 expression in OSCC, x100 and x400. C E: High levels of CDC20 expression in OSCC, x100 and x400. The scale bar is indicated at the left lower corner of each figure. 27

Figure 7: Univariable Kaplan-Meier analysis of cause-specific survival in oral squamous cell carcinoma patients. High CDC20 expression was associated with low overall survival in OSCC patients. 33

Figure 8: Univariable Kaplan-Meier analysis of cause-specific recurrence-free survival in oral squamous cell carcinoma patients. High CDC20 expression was not associated with recurrence- free survival in OSCC patients. The vertical lines and the "x" signals indicate the censored events. 34

Figure 9: Depletion efficiency of CDC20 protein by RNAi. Images obtained by immunofluorescence of HeLa cells at prometaphase with anti-CDC20 (red) and anti-α-tubulin (Green) staining; The DNA (blue) was stained with DAPI. In the control situation (CTR) there is a strong staining of CDC20 in kinetochores that is undetectable in cells after CDC20 depletion (siCDC20). Bar = 5µm. 39

Figure 10: Depletion of CDC20 protein induces an accumulation of cells in mitosis and cell death. Images obtained by phase contrast microscopy of HeLa cells in culture. 72 hours after CDC20 depletion (siCDC20), a considerable increase in mitotic cells (round configuration) is visible comparatively to the control situation (CTR). 96 hours after CDC20 depletion, the mitotic cells seem to undergo cell death (black arrow), a phenotype non-observable in the control situation. Bar = 40 µm. 41

Figure 11: Depletion of CDC20 protein induces an accumulation of cells in mitosis and cell death. Fluorescence microscope images from cytospin 72 hours after depletion of CDC20. A: transfected cells show an increase of cells arrested in mitosis with condensed chromosomes (white arrow) compared to the control situation. B: presence

of micro-nucleus (white arrow) indicating cell death after depletion of CDC20. Bar = 10 µm. 42

Table Index

Table 1: Association between CDC20 expression and clinicopathological characteristics in patients with oral squamous cell carcinoma 29

Table 2: Univariable analysis of cancer-specific and recurrence-free survival at 3 years, according to clinicopathological characteristics and CDC20 expression in oral squamous cell carcinoma patients 32

Table 3: Multivariable analysis of cancer-specific survival on variables with significant independent effect, according to tumor grade, N status, clinical stage, treatment modality, T status and CDC20 expression in oral squamous cell carcinoma patients ... 35

Table 4: Multivariable analysis of recurrence-free survival on variables with significant effect, according to T status, clinical stage, N status, treatment modality and gender in oral squamous cell carcinoma patients 36

Abstract

Chromosome segregation during mitosis requires the activity of the anaphase-promoting complex/cyclosome (APC/C), an E3 ubiquitin ligase that targets critical cell cycle regulators for degradation. Cell division cycle 20 (CDC20) is a crucial protein responsible for APC/C substrate recognition, namely securin and cyclin B, thereby allowing for triggering mitosis exit at the metaphase to anaphase transition. Overexpression of CDC20 protein was observed in several cancer types, including Oral Squamous Cell Carcinoma (OSCC). However, the clinical significance of CDC20 expression in OSCC patients has not been studied.

The present study aimed to analyze the CDC20 protein expression in tissues of patients with OSCC, relate them to clinicopathological characteristics and evaluate CDC20 potential as a prognostic biomarker and as a therapeutical target. Using tissue microarray technology, CDC20 expression was analyzed in 65 primary OSCC tissues by immunohistochemistry. Statistical analysis was performed to evaluate the clinicopathological and prognostic significance of CDC20 expression in OSCC. In order to evaluate the potential of CDC20 as a therapeutical target, interference RNA technique was used for CDC20 depletion and immunofluorescence technique was used to analyze the resultant phenotype.

Our results revealed that of the 65 cases of patients with OSCC studied, 37 (56.9%) showed high CDC20 protein expression and importantly, in univariable analysis, OSCC patients with higher CDC20 protein expression showed significantly shorter cancer-specific survival rate ($P = 0.018$). Multivariable analysis identified high CDC20 expression as an independent prognostic factor ($P = 0.032$). Therefore, high CDC20 expression is associated with poor prognosis in OSCC and may be used to identify high-risk OSCC patients. In HeLa cell line, the depletion of CDC20 gene expression led to an increase in the number of cells arrested in mitosis with condensed chromosomes and cell death, indicating that CDC20 may be a good target for OSCC treatment.

Resumo

A segregação dos cromossomas durante a mitose, requer a atividade de uma ubiquitina ligase E3, o complexo promotor da anafase/ciclossoma (APC/C), que encaminha importantes proteínas reguladoras do ciclo celular para a degradação. Cell division cycle 20 (CDC20) é uma proteina crucial responsável pelo reconhecimento de substratos pelo APC/C, nomeadamente a securina e a ciclina B, permitindo a transição de metafase para anafase e, consequente, a saída de mitose. Uma sobre-expressão da proteína CDC20 é observada em diversos tipos de cancro, incluindo o carcinoma oral de células escamosas (OSCC). No entanto, o significado clínico da expressão de CDC20 em pacientes com OSCC ainda não foi estudado.

O presente estudo, teve como objetivo analisar a expressão da proteína CDC20 em tecidos de pacientes com OSCC, relacioná-los com características clínicopatológicas e avaliar a CDC20 como potencial biomarcador de prognóstico e como alvo terapêutico. Usando a tecnologia de microarray de tecidos, analisamos a expressão de CDC20 em 65 tecidos primários de OSCC por imuno-histoquímica. A análise estatística foi realizada para avaliar o significado clínicopatológico e prognóstico da expressão de CDC20 em OSCC. De modo a avaliar o potencial da CDC20 como alvo terapêutico, foi utilizada a técnica de RNA de interferência para promover a sua depleção e foi utilizada a técnica de imunofluorescência para analizar o fenótipo resultante.

Os nossos resultados revelaram que dos 65 casos estudados de pacientes com OSCC, 37 (56,9%) apresentaram uma elevada expressão da proteína CDC20. Não foi verificada nenhuma correlação entre a expressão de CDC20 e nenhuma das características clínicopatológicas. No entanto, na análise univariada, os pacientes com tumores com elevada expressão da proteína CDC20 mostraram significativamente uma menor taxa de sobrevivência (P = 0,018). A análise multivariada identificou a elevada expressão de CDC20 como um fator de prognóstico independente (P = 0,032). A elevada expressão de CDC20 está associada a um mau prognóstico em OSCC e poderá ser usada para identificar pacientes com tumores de alto risco. Na linha celular HeLa, a depleção da expressão da proteína CDC20 revelou um aumento de células paradas em mitose com cromossomas condensados e morte celular, indicando que a CDC20 poderá ser um bom alvo terapêutico para o tratamento do OSCC.

Abbreviations

- APC/C: anaphase complex promotor/cyclosome
- BSA: bovine serum albumin
- Bub: budding uninhibited by benzimidazole
- BubR: bub1-related protein
- ºC: degree celsius
- CDC20: cell division cycle protein 20
- Cdks: cyclin-dependent kinases
- CENP-E: centromere–associated protein E
- CO2: carbbone dioxide
- CSS: cancer-specific survival
- CTR: control
- DAB: 3,3'-diaminobenzidine
- DAPI: 4', 6-diamidino-2-phenylindole
- D-MEM: dulbecco's modified eagle medium
- DMSO: dimethylsulfoxide
- DNA: deoxyribonucleic acid
- EDTA: ethylenediaminetetraacetic acid
- FBS: fetal bovine serum
- HCl: hydrogen chloride
- H_2O_2: hydrogen peroxide
- HRP: horseradish peroxidase
- KCl: potassium chloride
- KDa: kilodalton
- K_2HPO_4: dipotassium phosphate
- LI: labeling index
- M: molar (mol dm^{-3})
- Mad: mitotic arrest deficient
- MCC: mitotic checkpoint complex
- µg: micrograms
- µl: microlitres
- ml: millilitres
- mM: millimolar
- mm: milimeters
- nm: nanometer
- MPF: mitosis promotor factor
- MPS1: monopolar spindle 1
- MTAs: microtubule-targeting agents
- MTOCs: microtubule organizing centers
- NaCl: sodium chloride
- $NaHPO_4$: sodium phosphate
- OSCC: oral squamous cell carcinoma
- PFA: paraformaldehyde
- PSA: ammonium persulfate
- PBS: phosphate buffered saline
- PBS-T: PBS + Tween
- Rb: retinoblastoma protein
- RFS: recurrence-free survival
- RNA: ribonucleic acid
- RNAi: interference RNA
- rpm: rotations per minute
- SAC: spindle assembly checkpoint
- SDS: sodium dodecyl sulphate

- SDS-PAGE: sodium dodecyl sulfate – polyacrylamide gel electrophoresis
- siRNA: small interfering RNA
- TBS: tris-buffered saline
- TBS-T: TBS + Tween 20
- TEMED: N,N,N’,N’-tetramethylethylenediamine
  Tris: Tris-(hydroxymethy) aminemeth
- TMA: tissue microarray

Introduction

Cancer is one of the scariest diseases that affect people worldwide, independently of age or gender, and nobody is safe from this illness. The traditional therapies are painful with many side effects and most of the affected have low overall survival, so new therapies are urgently needed. Every day, scientists all over the world try to find the best therapy but this malignity is so complex that makes it hard to do so.

In the last decades, the cell cycle and its mechanisms have been studied in large extension due to its implication in several important processes such as growth, proliferation, regeneration and carcinogenesis. The new goal for cancer therapy is targeting the proliferative capacity of cells. It has been proposed that targeting mitosis is an efficient strategy [5]. Specifically, the spindle assembly checkpoint (SAC) has recently been suggested as a promising anti-cancer target [6]. Therefore, an exhaustive understanding of the biological and molecular phenomena that characterize mitosis can be a start point on therapy personalization, being for this reason, a currently active target of investigation. In this context, the present work focuses on oral squamous cell carcinoma, considered a worldwide health concern, in which cells frequently exhibit aneuploidy, suggesting defects in spindle assembly checkpoint.

The following section contextualize the work presented in this thesis, starting with a brief description of the cell cycle and the two major stages that characterize it, the interphase and mitosis, as well as its regulation and control mechanisms. Subsequently, concepts and mechanisms related to the progression of mitosis are revised, focusing on the mechanism of spindle assembly checkpoint and some defects around this process. Lastly, a brief review is made on the currently known aspects of OSCC and CDC20 expression and behavior on this disease.

1. The cell cycle

The cell cycle is an essential and balanced process that allows the reproduction and development of all living organisms. It includes an ordered sequence of discrete stages controlled by complex molecular interactions to produce two genetically equal daughter cells [7, 8]. In eukaryotic cells, it consists of two major events in a temporally regulated fashion: DNA synthesis (Interphase) and the chromosome segregation (Mitosis), culminating in two completely individualized cells, a phenomenon named cytokinesis.

The interphase represents the most part of the cell cycle time comprising orderly transitions from G_1, S to G_2 phase. The G1 phase corresponds to the gap between mitosis ending and beginning of DNA synthesis [9]. During this phase, the cell is

sensitive to extra and intercellular signals which determine the cell fate, whether to divide itself or to remain in quiescence stage (G0 phase). Non-dividing cells or cells unable to enter the cell cycle or in a temporarily arrest state, remain in G0 phase. Once initiated the cell progression, the cell grows and prepares for DNA replication on the subsequent phase, the S phase [10-12]. Afterwards, on G_2 phase, the cell grows continuously and essential proteins and enzymes are synthesized for genomic separation on mitosis [2, 13-15].

2. Mitosis

Comparatively to interphase, mitosis requires much less time to occur and ensures accurate transmission of genetic inheritance, as well as one centrosome and cellular organelles into each daughter cell, making it the most critical event of the cell cycle [16, 17]. The correct genetic material transmission during mitosis depends on efficient execution of two previous events during interphase: the replication of chromosomal DNA and centrosome duplication [16, 18]. Classically, mitosis can be divided into five subphases – prophase, prometaphase, metaphase, anaphase and telophase – that ends with cell division (cytokinesis).

At prophase, the chromatin condensation begins and the replicated centrosomes move towards the opposite poles of the cell. The centrosomes have the ability to nucleate and organize microtubules and, for this reason, they are known as the primary microtubule organizing centers (MTOCs), in higher eukaryotic cells [19]. The prometaphase, an extremely dynamic cell cycle phase, is initiated by nuclear envelope breakdown and chromosomes dispersion into the cytoplasm. The chromosomes include specific constriction regions called centromere that provides the foundation for kinetochore assembly and these, in turn, form a dynamic interface with the microtubules from the mitotic spindle [20]. This way, the kinetochore is a core multiprotein structure, that mediates chromosomes attachment to the mitotic spindle and the monitoring of those attachments, chromosome transportation to spindle poles and arrest of cell cycle if defects are detected, through the initiation of a signaling checkpoint pathway [18]. After nuclear envelope breakdown is completed, each chromosome initiates the biorientation process and moves to the equatorial plate through microtubules that grow and shorten by association and disassociation of α/β-tubulin heterodimers, respectively [21].

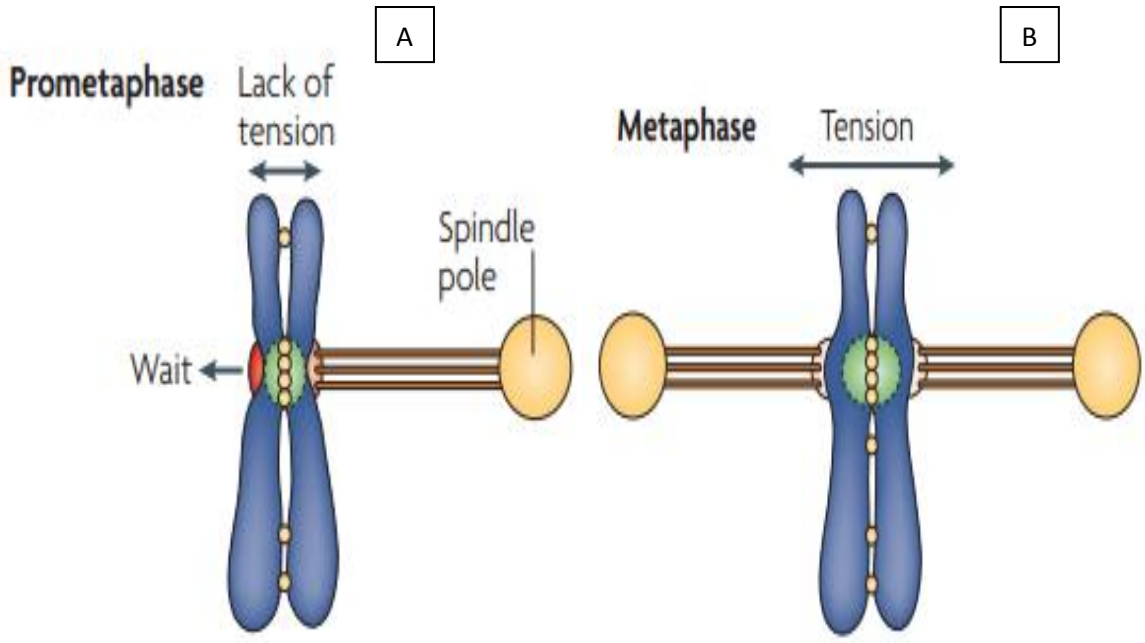

Figure 1: Kinetochore-microtubule interactions. A: during prometaphase, one sister chromatid is attached to microtubule from only one spindle pole (monotelic attachment) and a wait signal is generated. B: at metaphase, both sister chromatids become attached to microtubules from both spindle pole (amphitelic attachment) with the appropriate tension [3]

During the kinetochore-microtubules attachment process, chromosomes initially become mono-oriented (monotelic attachment) by one sister kinetochore and moves, through microtubules, toward one spindle pole and they are not under tension (figure 1 A). Subsequently, the other sister kinetochore is captured by microtubules from the opposite pole and the chromosome becomes bi-oriented (amphitelic attachment) in equatorial zone, as exemplified in figure 1 B [18, 22, 23]. The tension developed across the paired kinetochores pulls the sister chromatids toward two opposite poles [24]. On metaphase all chromosomes must have proper bipolar attachment and be correctly aligned on the metaphase plate. Once bi-orientation of all chromosomes is achieved, the cell enters anaphase. Sister chromatid cohesion is lost by centromere disorganization and spindle elongation, resulting in separation of sister chromatids to opposite poles [17]. When chromosome separation is completed, nuclear envelope is reorganized and chromosomes decondense into their interphase conformations on telophase. Finally, in

cytokinesis, a contracting ring composed of actin-myosin cleaves the cytoplasm and originates two daughter cells [9, 12]. These processes are exemplified in figure 2.

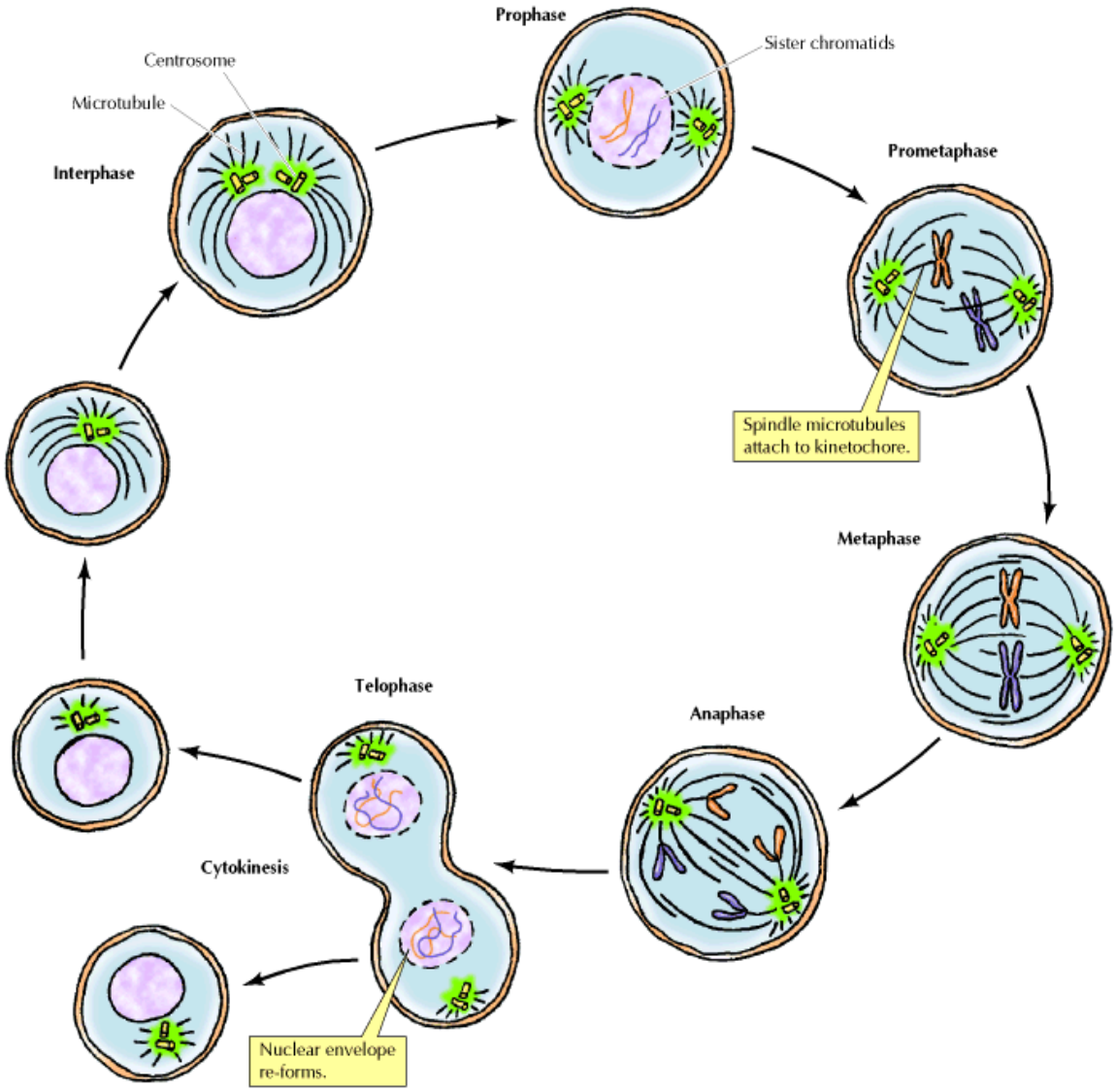

Figure 2: Representation of mitotic phases. At the end of prophase the chromosomes are condensed and the matured centrosomes move towards the opposite poles. During the prometaphase the kinetochores are captured by microtubules from mitotic spindle. At metaphase the chromosomes must be properly aligned at metaphase plate to allow sister-chromatid separation in anaphase. In telophase nucleus division occurs and is followed by two daughter cells' formation in cytokinesis [2].

3. Cell cycle regulation

Each phase of the cell cycle is executed during a precise predetermined time which provides high fidelity, otherwise it can lead to aneuploidy, an imbalance on chromosome number, or genetic instability. The cyclin-dependent protein kinases (cdks) are the regulatory proteins involved in this process [10, 16]. They are a family of serine/threonine proteins that act at precise points of the cell cycle and regulate the activity of specific proteins through phosphorylation., they require a cyclin for their activation [14] [25]. As illustrated in figure 3, they are associated with their correspondent cyclins during the different phases of cell cycle, namely G1 (cyclin D and E), S phase (cyclins A) and mitosis (cyclin A and B). The cyclins levels are changed periodically during the cell cycle [26], therefore, the regulation of the concentration of cyclins determines the activity of Cdks. Cell cycle progression depends on the balance between the different cyclin-CDK complexes [2].

When the cell fulfils the requisites to exit from the quiescence stage to proceed in the cell cycle, cyclin D is the first cyclin to be expressed during the presence of growth factor stimulation. Cyclin D, in association with Cdk 4 and Cdk 6, enters the nucleus and contributes for retinoblastoma protein (pRb) phosphorylation. This stimulates the activation of the E2F family of transcription factors and the transcription of fundamental proteins essential for G1 and S phase. Afterwards, the cyclin E associated to Cdk 2 is responsible for transition from G1 to S phase supporting DNA replication regulation [2]. Cyclin A is expressed immediately following cyclin E and, in association with Cdk2, becomes essential during S phase. It is important for initiation and completion of DNA replication, as well as to ensure that this phenomenon occurs only once in each cell cycle. Its levels remain high until the onset of mitosis to contribute to chromosome condensation [27]. The progression through the G2 phase and entry into mitosis is mediated by Cdk1-ciclina B complex named “mitosis promoting factor” (MPF). In mitosis, MPF promotes nuclear and cytoplasmic changes such as chromosome condensation, nuclear envelope breakdown, fragmentation of Golgi apparatus and spindle formation [2].

When cyclins have completed their function in the cell cycle, they must be degraded by the 26S proteosome. Cyclin B and A destruction, during mitosis, is essential to promote cell return to interphase and the possibility of a new cell cycle [26].

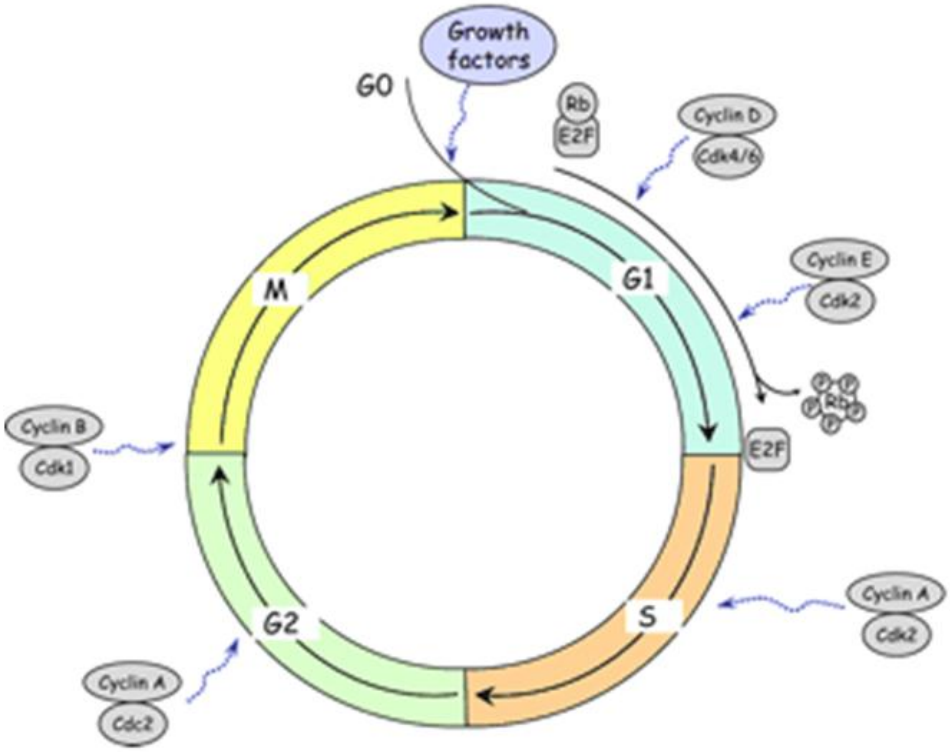

Figure 3: Cell cycle regulation by cyclin-dependent protein kinases (Cdks). Schematic representation of cdks involved in progression of the cell cycle. The cyclin D-Cdk4/6 complex controls the cell cycle entry, the cyclin E-Cdk2 complex promotes the initiation of DNA replication, the cyclin A-Cdk2 complex stimulates DNA replication and lastly, the cyclin B-cdk1 complex is essential for entry and progress of mitosis (Adapted from [4]).

4. The spindle assembly checkpoint

The coordination between the different phases of the cell cycle and the assurance that each phase is performed in the right order is assured by specific checkpoints that are specialized control points. These checkpoints prevent the passage to the next phase until the events of the last one are properly completed without errors [2]. Globally, their role is to detect unreplicated or damaged DNA across G1, S and G2 phase and chromosome misalignment in mitosis. In the presence of an error, the cell cycle is arrested or delayed by these checkpoints allowing time to correct the mistake. However, if the mistake is irremediable, the cell is committed to apoptosis [28].

For instance, in case of DNA damage during G1 phase, the cell is arrested by the action of p53 protein that allows p21 protein transcription. Consequently, p21 will

inhibit the cyclin/Cdk complex activity preventing pRb phosphorylation, which remains bound to E2F and cell is not able to proceed to S phase [29]. In G2 phase, if DNA condensation or integrity isn't complete, a checkpoint is activated and the Chfr protein is free to phosphorylate cdc25 protein, promoting its inhibition. This way, cdc25 is not able to activate MPF, resulting in cell arrest in G2 [30, 31].

The spindle assembly checkpoint (SAC) is a crucial surveillance mechanism with a complex signaling cascade continuously active that is in charge for the control of mitosis. It monitors the kinetochore-microtubule interactions and delays the anaphase onset until all chromosomes are properly attached to microtubules from mitotic spindle, bi-oriented and aligned in metaphase plate, ensuring an equal segregation of the genome into each daughter cell [3, 32].

4.1 Molecular pathway of the SAC

The molecular pathway of the SAC, that promotes an inhibitory signal to prevent premature sister-chromatid separation, involves the function of highly conserved proteins, such as Bub1, BubR1, Bub3, Mad1, and Mad2 representing the bona fide SAC proteins. The Mad (mitotic arrest deficient) and Bub (budding uninhibited by benzimidazole) proteins families were first identified by genetic screens in budding yeast [33]. These proteins accumulate at kinetochores of chromosomes that are not bi-oriented preventing premature chromosome separation. MPS1 (monopolar spindle 1) also plays an important role in the SAC. Homologues for these proteins have been identified in mammals and have been proven to share a high degree of both sequence and functional homology with their yeast counterparts [33, 34].

Other SAC proteins were identified in higher eukaryotes include the Aurora kinase B, the centromere–associated protein E (CENP-E), dynein and the Zw10-Rod-zwilch protein complex. Aurora kinase B activity is important for kinetochores that are not under the appropriate tension, that normally is achieved by forces from bipolar attachments [17]. In turn, the CENP-E regulates the SAC by acting on BuBR1 and is essential for kinetochore microtubule attachments. The dynein is responsible for movement toward the (−) end of microtubules and the Zw10-Rod-zwilch protein complex interacts with it [12].

The main target of SAC is the cell division cycle 20 homolog (CDC20) protein, an activator of the anaphase-promoting complex/cyclosome (APC/C). This complex is a multi-subunit E3 ubiquitin ligase that targets proteins for degradation that are essential

for anaphase onset [33, 35]. As long as there are improperly attached or unattached chromosomes, the SAC will be active and an inhibitory complex will be generated, called “mitotic checkpoint complex” (MCC) that comprises the SAC Mad2, Bub3, Bub1, BubR1 proteins and the mitotic exit regulatory protein CDC20. This way CDC20 is sequestered and prevented from activating the APC/C [36-39] (figure 4A).

Once all chromosomes become aligned at the metaphase plate, the MCC complex disassembles and SAC is silenced. CDC20 can then bind and activate the APC/C which targets securin and cyclin B for proteolysis by the 26S proteosome [40]. Destruction of securin leads to release and activation of separase which cleaves Scc1, one important component of the cohesin complex holding sister-chromatids together, resulting in sister chromatid separation and anaphase onset [41, 42]. Cyclin B degradation promotes exit from mitosis into the subsequent interphase by inactivation of cyclin-dependent kinase 1 (Cdk1) [36, 38, 43] (figure 4B).

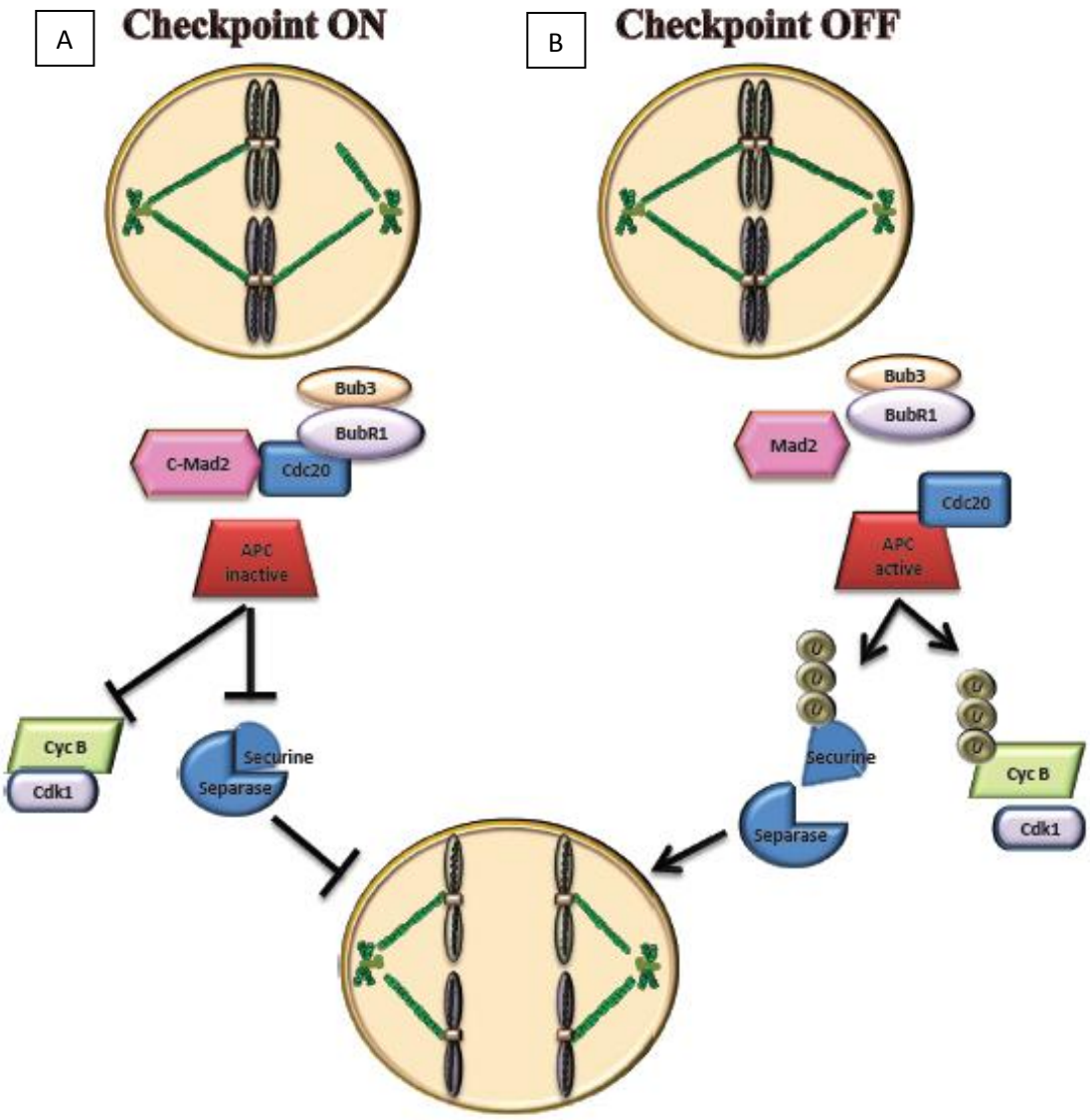

Figure 4: Molecular pathway of spindle assembly checkpoint (SAC). A: The presence of unattached or improperly attached chromosomes leads to SAC activation. An inhibitory signal is generated by the mitotic checkpoint complex (MCC) comprised by BubR1, Bub3 and Mad2. CDC20 is sequestered and the APC/C remains inactive preventing securin and cyclin B degradation and the cycle is arrested. B: When all chromosomes are properly aligned in metaphase plate the SAC is silenced. CDC20 is free to bind and activate the APC/C that targets securin and cyclin B to proteolysis. Securin degradation leads to separase activation and sister-chromatid separation. Cyclin B degradation results in mitotic exit [1].

4.2 SAC defects in cancer

Nowadays, it is acknowledged the presence of high frequency of genetic instability in cancer. This genetic instability can result in aneuploidy that is defined by the gain or loss of chromosomes caused by defects in chromosome partitioning through mitosis and it is a distinctive feature in several cancer types, mainly in most solid tumors [44, 45]. In normal cells, the process across segregation of genetic material to daughter cells has a low error rate due essentially to the high fidelity of SAC. Nevertheless, in tumor cells this surveillance mechanism is mostly compromised and it has been suggested as aneuploidy cause [17, 44]. This is expected because if the SAC is weakened, the cells can eventually proceed to anaphase with one or more misaligned chromosomes which leads to missegregation and consequently to aneuploidy [46, 47], as shown in figure 5. It has also been suggested that cells with a weakened SAC have higher carcinogenic potential than cells with an effective SAC [48]. Although SAC genes mutations are rare, the detection of changes in the expression levels of SAC genes is very frequent in tumor cells [34, 49].

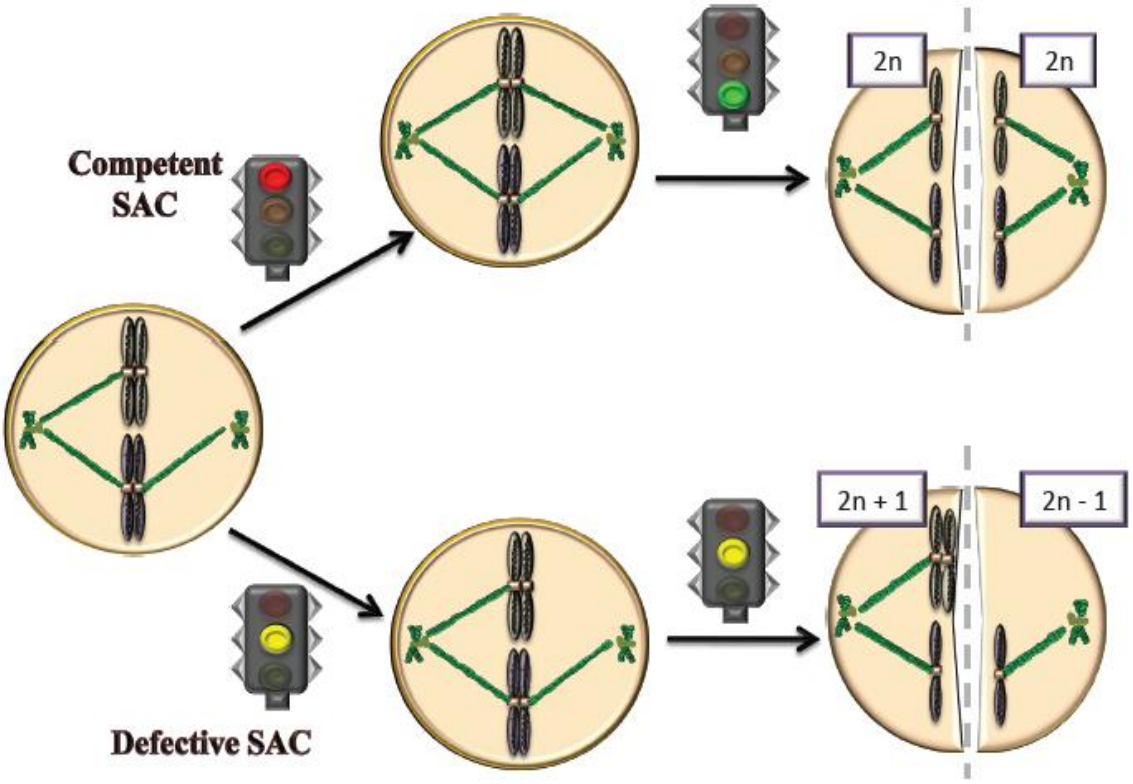

Figure 5: A defective SAC can lead to aneuploidy. In normal cells with a competent SAC, the chromosome missegregation is prevented. In cell with a defective SAC, the residual checkpoint activity is sufficient to ensure the accuracy of chromosome segregation [1].

Many studies were carried out in order to establish the relationship between SAC defects and tumor development. In some colorectal cancer cell lines, heterozygous mutations were identified in Bub1 and BubR1 [50] and also seen in diverse B cell lymphomas [51]. Likewise, mutations in the Mad2-enconding gene were found in breast and gastric cancer cell lines [52]. Mutations in Mad1L1 gene were reported in 44 cell lines and in 133 primary cancer samples [53]. Moreover, it was reported that a point mutation in the *hBUB1* gene suggests the hypothesis that alteration of mitotic checkpoint genes is involved in the development of primary lung cancers [54].

However, in several tumors where genetic instability was reported, mutations were not detected in any SAC gene, which strongly indicates that they may not play a central role on tumorigenesis. Nevertheless, changes in expression levels of these genes have already been found in numerous cancers such as breast, colorectal, ovarian, lung and

oral cancer, among others [45, 55]. It has been shown in several studies that the complete deactivation of SAC is lethal [56]. Thus, the dysregulation of SAC, and not its complete ablation, is commonly seen in many cancers [56, 57].

In mice with reduced BubR1 expression levels the incidence of tumor increased [58]; BubR1 haploinsufficiency in mice and the downregulation of this protein by interference RNA result in tumor development [59]. On the other hand, BubR1 overexpression was found in hepatocellular [60] and squamous cell carcinomas [61].

Reduced Mad2 expression levels in mice demonstrated high incidence of lung tumors [33] and has been implicated in human hepatocellular carcinogenesis [62]; Furthermore, Mad2 knockdown by interference RNA in normal human fibroblasts and other cell lines leads to chromosome missegregation and mitotic catastrophe [57, 63] and, in a gastric cancer cell line, its depletion enhance drug resistance and cell proliferation [64]; In turn, Mad2 overexpression has been shown to promote genomic instability in cell cultures [65] and can initiate tumorigenesis [66].

The overexpression of Bub1, Bub3 and BubR1 was reported in human gastric cancer [67] and recently, it has been shown that the Mad1 high expression levels lead to chromosomal instability and resistance to anti-microtubules drugs [68].

Defective SAC signalling that is compatible with tumor cell survival appear to contribute to the development of aneuploidy, a crucial factor for tumor cell evolution. The existence of differences on SAC regulation between normal and tumor cells could be a potential strategy target to kill tumor cells without affecting normal cells [49].

5. Targeting the SAC as a cancer therapy strategy

Nowadays, anti-cancer drugs include molecules that inhibit the hyperproliferation of tumor cells by targeting cell cycle and subsequent induction of apoptosis. The mitotic drugs in clinical use named microtubule-targeting agents (MTAs) such as microtubule-stabilizing (taxanes) and microtubule-destabilizing drugs (vinca alkaloids), have been efficient in a wide range of cancer types for many years [69]. These two classes of drugs inhibit the microtubules' dynamics, which is the key for the movement and alignment of chromosomes in the metaphase plate promoting the spindle assembly checkpoint activation, which leads to cell arrest and apoptosis [5, 6, 21]. Besides their benefit in cancer therapy by targeting actively dividing cells, they have undesirable side effects by disruption of important physiological pathways observed in normal cells. Neurological and hematological side effects are the most important. Drug resistance is also a common

problem. Moreover, tumor cells do not have an efficient SAC that fully respond to mitotic errors which compromises the complete effectiveness of MTAs. In this sense, there is active research for new mitotic drugs with higher specificity and fewer side effects [70-72].

The current understanding of the SAC molecular pathway provides their use for strategy therapy design in cancer. Small molecule inhibitors against SAC proteins are already being developed [71]. For instance, interfering with Aurora B kinase results in 98% reduction in tumor volume through decrease in viability of rapidly dividing cells in nude mice injected with human leukemia cells [72]. The inhibition of chromosome alignment and cytokinesis is the major phenotype for Aurora B kinase inhibition resulting in severe polyploidization. Several small molecule against this protein are already under development in clinical trials [73]. Moreover, patents of oligonucleotides or peptides against BubR1, Bub3 and Mad2 have already been approved [72], as well as against CENP-E, which results in a mitotic delay with misaligned chromosomes followed by apoptosis [74].

6. SAC components as cancer biomarkers

In recent years, advances have been made in the efficiency of detection and efficacy of cancer treatment through the improving of the knowledge on biomarkers in cancer. These biomarkers provide a tool for measuring and evaluating normal biologic and pathogenic processes or pharmacologic responses to a therapeutic intervention [75].

Biomarkers are used with the aim of identifying high risk populations, diagnosing in early stages, selecting the best treatment and monitoring the response to treatment [75]. Some SAC components are seen as important biomarkers. For instance, a high BubR1 expression in gastric cancer cell lines is correlated significantly with DNA aneuploidy, tumor invasiveness, lymph node metastasis, liver metastasis and poor prognosis [76]. Furthermore, it has been showed recently that overexpression of Mad2 predicts clinical outcome as a crucial prognostic factor in primary lung cancer patients [77]. The overexpression of Aurora B was found to be an effective predictor of aggressive epithelial ovarian carcinoma in terms of differentiation, metastasis and prognosis [78]. In addition, Aurora B expression has been associated increased with cell proliferation and poor prognosis in non-small cell lung carcinoma [79] and hepatocellular carcinoma [80].

Recently, CDC20 has also been seen as a biomarker in pancreatic ductal adenocarcinoma with an important role in disease tumorigenesis and progression [81] and, furthermore, it was identified as an independent prognostic factor in primary non-small cell lung cancer patients [82].

The discovery of new biomarkers and the understanding of their relevance will be very important for an efficient disease diagnosis and, consequently, for the choice for the appropriated therapy, in order to benefit the patients [75].

7. The oral cavity cancer and SAC

Oral squamous cell carcinoma (OSCC) is the most common head and neck cancer and represents a major world health problem with an incidence of more than 300,000 cases annually [83]. It is acknowledged that oral cancer occurrence differs according to age, ethnic group, life habits and culture [84]. The Indian population shows the highest incidence and prevalence of this type of cancer because of the common habits of chewing tobacco, which, in parallel with alcohol, is the most important risk factor [85].

OSCC shows a weak prognosis and high morbidity, with a 5-year survival rate of 50% which has not changed significantly during the last decades. This low survival rate is due essentially to identification of lesions on advanced stage or the appearing of metastasis or tumor recurrence [86]. OSCC patients have a good prognosis and outcome if the diagnosis and treatment of the disease are made in an early stage, but this is difficult since the lesions are always asymptomatic. Only with the development of the disease the lesions became symptomatic because of the involvement of nerves [87]. Moreover, in an advanced stage, the quality of the patient's life is compromised due to higher radio-, chemo- and surgical therapy that often lead to significant physical effects on patients [84].

Like the main cancer types, OSCC also exhibits aneuploidy which suggests defects in spindle assembly checkpoint [83] [88]. Indeed, it is known that this malignity is associated with an overexpression of CDC20, as well as Bub1, BubR1 and Bub3 [89, 90]. In addition, it was show that the aurora B expression is correlated with cell proliferation, histologic differentiation, and metastasis, and that BubR1 overexpression may be involved in progression of OSCC [61, 89].

8. CDC20 expression in OSCC

Cell division cycle 20 homolog (CDC20) is the main target of the branch of the SAC that interacts directly with the anaphase-promoting complex/cyclosome (APC/C), which triggers the degradation of cyclin B and securin resulting in anaphase initiation and mitosis progress. This protein is kept sequestered during prophase and metaphase by the mitotic checkpoint complex (MCC) to prevent premature exiting from mitosis, until the attachment of all kinetochores to their respective spindle poles.

CDC20 has seven WD40 repeat regions at its C-terminus, forming a β-propeller structure that is specialized for protein-protein interaction. During the mitotic arrest in human cells, CDC20 is continuously synthesized and degraded with a half-life of around 30 minutes. Once CDC20 binds to APC/C complex, it becomes a substrate for ubiquitination and subsequent degradation, thus its levels are strongly controlled through equilibrium of translation and degradation. Moreover, a careful balance between the levels of CDC20, BubR1 and Mad2 proteins must be maintained for a functional SAC; some studies reported that changes in the ratio between CDC20 and BubR1/Mad2 result in SAC defects [91].

Indeed, overexpression of CDC20 was observed in several cancer types, including tumor of the oral cavity [90], stomach [92], pancreas [81], lung [93] and brain (glioblastoma) [94].

Interestingly, studies reporting overexpression of CDC20 in OSCC also suggested that such overexpression can deregulate APC/C activation and result in premature anaphase onset and aneuploidy, consistent with a role of CDC20 in oral tumorigenesis [90]. However, until nowadays, the clinical significance of CDC20 expression in OSCC patients has not been studied.

Aim of the study

Oral squamous cell carcinoma (OSCC) is among the most common cancers worldwide and has a poor 5 year survival rate. Tools that can differentiate lesions with higher risk of conversion to malignancy compared to lesions with relatively lower risk are a promising therapeutic strategy for this malignity. Several genetic lesions have been implicated in oral cancer, including tumor suppressors like TP53 and RB, and oncogenes like cyclin family, EGFR, and ras. However, the molecular model of oral carcinogenesis remains to be elucidated. Therefore, further comprehension of the molecular basis of oral cancer is needed not only to understand its multi-step progression but also to supplant traditional markers and to develop potential therapeutic interventions.

Like in many other tumours, the OSCC exhibit aneuploidy and it has been reported the presence of spindle assembly checkpoint (SAC) defects as a potential cause. The SAC ensures the correct execution of mitosis preventing genetic instability. CDC20 is responsible for the anaphase-promoting complex/cyclosome (APC/C) activation which is required for mitotic exit. This protein is the main target of the SAC and is sequestered to prevent premature exit from mitosis when the chromosomes are not properly attached to microtubules of the mitotic spindle and aligned at the metaphase plate.

Given the role of CDC20 in mitotic exit, many studies were carried out in order to establish a causal connection between CDC20 expression deregulation and tumor development. Accordingly, overexpression of CDC20 was observed in several cancer types, including Oral Squamous Cell Carcinoma (OSCC). However, the clinical significance of CDC20 expression in OSCC patients has not been studied. Therefore, the aims of the present study were: i) to analyze CDC20 protein expression in tissues from patients with OSCC; ii) to relate CDC20 expression to OSCC clinicopathological characteristics; iii) to evaluate CDC20 potential as a prognostic biomarker; and iv) to evaluate CDC20 as a therapeutical target.

Material and methods

Tissue microarray (TMA) construction

For tissue microarrays (TMA), tumor tissues from sixty five patients diagnosed and treated for primary OSCC at the Hospital de Santo António (HSA), Porto, Portugal, between 2000 and 2006, were included. Representative tumor areas were selected on haematoxylin and eosin-stained sections and marked on paraffin blocks. Three 2 mm cylindrical tissue cores were obtained from each selected specimen and transferred to a recipient paraffin block, using a microarray instrument (TMA Builder, Histopathology Ltd, Hungary). From each TMA block, 3-µm sections were cut and processed for immunohistochemistry.

Immunohistochemistry

TMA slides were deparaffinized in xylene followed by antigen-retrieval treatment with 0.01M citrate buffer (pH 6.0) in a 98°C water bath for 30 min. After blocking endogenous peroxidase with methanol containing 0.3% hydrogen peroxide (H_2O_2) for 15 min, sections were incubated with a blocking solution made of 0.4% casein in tris-buffered saline (TBS) to reduce nonspecific binding. Slides were incubated with anti-CDC20 mouse monoclonal primary antibody (clone p55 CDC (E-7); sc-13162, Santa Cruz Biotechnology, Santa Cruz, CA) at 1:50 dilution in TBS for 1 hour at room temperature in a humidified chamber. Slides were then washed in TBS, after which primary antibody was detected using a standard peroxidase-labeled dextran polymer for visualization with 3,3'-diaminobenzidine (DAB) as chromogen (NovoLinkTM Polymer Detection System; Novocastra, Leica Biosystems Newcastle Ltd), according to the manufacturer's instructions. Finally TMA sections were counterstained with Mayer's haematoxylin. In each staining run, we used endothelial cells as positive control [94] and omission of primary antibody as negative control.

Evaluation of immunohistochemistry

CDC20 expression was evaluated on the basis of the percentage of nuclear positivity for CDC20 protein and it was done independently by two different investigators. CDC20 labeling index (LI) was determined using the formula below:

$$\text{Labeling index (LI)} = \frac{\text{CDC20 positive}}{\text{CDC20 positive} + \text{CDC20 negative}} \times 100$$

At least 150 nuclei were counted in each case. To determine the cut-off of CDC20 protein expression, it was included ten cases of normal oral mucosa (buccal mucosa, and gengiva) within TMA. Their labeling index mean was 7.5±1.28 (range 5-9). According to this result, a cut-off of 10% was set as the threshold of positive cells with CDC20 expression. CDC20 expression was graded as negative (proportion of positive cells <10%) or positive (proportion of positive cells >10).

Microscopy, image acquisition and processing

The images from immunohistochemistry assays were obtained with a 40x objective lens on a Nikon TE 2000-U microscope equipped with a DXM1200F digital camera through Nikon ACT-1 program. Photoshop CS5 (Adobe Microsystems, CA) was used to treat the final images.

Statistical analysis

Data were statistically analyzed using IBM SPSS Statistics version 20.0 software (IBM Corporation, NY, US). The associations between the different clinicopathological characteristics and Cdc20 levels were analyzed by Chi-square test. The cancer-specific survival (CSS) and recurrence-free survival (RFS) were estimated by the Kaplan-Meier method and their prognostic effect was tested using the log-rank test. Variables with significant effects in the univariable analyses were entered into Cox regression model to investigate their independent predictive significance. *P* value of less than 0.05 was considered significant.

Cell culture

The cell lines, HeLa (Human cervical carcinoma, Faculty of Pharmacy, University of Porto) and oral SCC25 (Squamous cell carcinoma, ATCC), were maintained at 37ºC in a humidified incubator (Hera Cell, Heraeus) with 5% of CO_2 and grown in monolayer in T25 flask (Nunclon™ Δ Surface) in DMEM (Dulbecco's Modified Eagle's Medium, GIBCO Invitrogen) and DMEM F12 medium (GIBCO Invitrogen), respectively. Both media were supplemented with 10% v/v of FBS (Fetal bovine serum, HyClone), 1% m/v of antibiotic-antimycotic (GIBCO Invitrogen) and 1% m/v of L-glutamine (GIBCO Invitrogen). DMEM F12 medium was also supplemented with hydrocortisone (40ng/mL, Sigma). At 80% confluence, cells were split into a new flask with fresh medium to avoid cell death due to lack of space or nutrients. For that purpose, the

medium was removed, the cell monolayer was washed with 2mL of phosphate-buffered saline PBS (pH 7.4: 137mM NaCl, 2.7mM KCl, 18mM K_2HPO_4, 100mM $NaHPO_4$) and incubated with 1mL of trypsin-EDTA (Gibco™, Invitrogen Corporation) for 3-10 minutes at 37ºC to promote detachment. Trypsin was then neutralized and cells were resuspended in warm medium. Cell density was determined by adding 30 µl of trypan blue solution to 30 µl of cell suspension and the cells were counted in a *Neubauer* chamber. Finally, the desired number of cells was transferred into a new flask with fresh medium and returned to the incubator.

Cell freezing and thawing

The cell freezing began with the detachment of log phase cells by trypsin-EDTA and centrifugation for 5 minutes at 1000 rpm. After that, $1x10^6$ to $2x10^6$ cells were resuspended in 1mL freezing medium (DMEM with 5% v/v of DMSO or DMEM F 12 with 10% v/v of DMSO) in a cryogenic vial and kept at - 80ºC in a recipient with isopropyl alcohol to allow a gradual cooling. After 24 hours, the vial was stored in liquid nitrogen.

For the thawing process, cryogenic vial from liquid nitrogen storage was quickly placed in a water bath at 37ºC for 1-2 minutes, and thawed cells were gently collected, put in a T25 flask containing warm medium, and kept in the incubator at 37ºC with 5% of CO_2. After 24 hours, the culture medium was changed to a fresh medium in order to remove any traces of DMSO.

Coating of glass coverslips with poly-L-lysine

The coverslips (22 x 22 mm, VWR) were covered with 1M HCL at 50-60ºC for 8-16 hours. Afterwards, they were washed vigorously in deionized water and then in 95% ethanol and left to dry. After that, the coverslips were put into Petri dishes containing Poly-L-lysine (500µl/mL) solution. After 1 hour of agitation, poly-L-lysine was removed, the coverslips were washed in distilled water and bi-distilled water 5 times each and left to dry. At the end, the coverslips were kept in a Petri dish wrapped in parafilm.

RNA Interference

HeLa and SCC25 cell lines were inoculated in a 6 wells plate at a density (number of cells per ml) of $0,03x10^6$ cells and $0,07x10^6$ cells in 1,5mL of culture medium with

5% of FBS. After 24 hours at 37ºC, two transfection reactions were prepared: 3µL of Oligofectamine with 15µl de Opti-MEM (Invitrogen) and 1µl of siRNA against Cdc20 (Quiagen) with 184,4µl de Opti-MEM (Invitrogen). The reaction mixes were homogenized and left at room temperature for 30 minutes. Afterwards, the transfection solution was gently added drop by drop to the cell-containing wells and incubated at 37ºC. The next day, the medium was changed to complete medium. 72 hours after the transfection, cells were processed for RNAi efficiency evaluation and phenotype analysis by immunofluorescence.

Cytospin

The slides were assembled with a paper filter and a cuvette in a metal holder. The medium from the 6 wells plate after RNAi, with most mitotic cells, was collected into a falcon as well as the detached cells. cell density was determined in a *Neubauer* chamber. A final volume of 200 µl with $0.05x10^6$ and $0.06x10^6$ cells per ml in HeLa and SCC25, respectively, was placed in each cuvette with 1 drop of 3% BSA. The samples were then spun at 800 rpm for 3 min. After 2 hours in air drier, the cells were fixed with 2% formaldehyde in PBS (1x) for 10 min and permeabilized with 0.1% of Triton X in PBS (1x) for 5 min (2 times). Finally, the slides were washed in PBS (1x) for 5 min and then mounted in Vectashield with DAPI (Sigma) at 0,5 µg/mL.

Immunofluorescence

The cell lines HeLa and SCC25 were inoculated in a 6 wells plate at a density (number of cells por ml) of $0,03x10^6$ and $0,07x10^6$, respectively. Cells were fixed in freshly prepared paraformaldehyde 2% (v/v) (sigma) PBS, for 7 minutes at a room temperature. Then, they were washed three times for 5 minutes in PBS, and permeabilized with a solution of Triton X-100 0.2% in PBS during 7 minutes. After that, they were washed in PBST (PBS, 0.02% Tween) three times for 5 minutes each. Cells were blocked with 10% of FBS in PBST for 1 hour in a humidified chamber and then incubated with the primary antibody: *rabbit* anti-Cdc20 (1:1000, sigma) and *mouse* anti-α-tubulin (1:2500, Sigma). The coverslips were washed three times in PBST during 5 minutes each and then were incubated with the secondary antibody with a dilution of 1:1500 (anti-*mouse* and anti-*rabbit* conjugated with 488nm or 568nm Alexa Fluor; Molecular Probes). Finally the cover slips were washed two times in PBST and one in PBS and then assembled in 7µl of DAPI.

Protein extraction and quantification

The cell suspension with the grown media initially recovered from culture flask, as well as the detached cells, was centrifuged at 4ºC, for 5 minutes, at 4000 rpm. The pellet was quickly resuspended with 150µL of cold lysis buffer (pH 7,5: NaCl 50mM; Triton X-100 0,5% (v/v); EDTA.Na 1mM; cocktail of protease inhibitors - Sigma) and transferred to an eppendorf. Then, the suspension was passed several times through a syringe and the lysates remained on ice during 20 minutes. The lysates were then centrifuged at 13000 rpm for 5 minutes at 4ºC. 10µl of the supernatant was used to measure the protein concentration, and the rest of the sample was frozen at - 80ºC for western blotting assays.

Protein quantification is essential to ensure an equitable loading between the samples in electrophoresis gel and require a standard curve using the kit "BCATM Protein Assay Kit" (Pierce Biotechnology, Inc). According to the kit, the work reagent was prepared by mixing 50 parts of BCA Reagent A (sodium carbonate; sodium bicarbonate; bicindroninic acid and sodium tartrate in 0.1M sodium hydroxide) with 1 part of BCA Reagent B (4% cupric sulfate). The protein samples to be quantified were diluted ten times in distilled water and its quantification was performed by spectrophotometric reading at 562 nm according to the instructions of the kit manufacturer.

Western blotting

5µg of HeLa or SCC25 protein extracts were separated in SDS-PAGE (sodium dodecyl sulfate polyacrylamide gel electrophoresis) and processed for western blotting. The SDS-PAGE consisted in a 6% staking gel and a 10% separating gel comprised by polyacrylamide 30%, de-ionized water, 1.5 M Tris pH 8.8 (resolving gel), 1.0 M Tris pH 6.8 (stacking gel), PSA 10%, TEMED and SDS 10%. A Mini-PROTEAN 3 system (Bio-Rad Laboratories) was used for electrophoresis assays filed with running buffer (25mM Tris HCl, pH 8.3; 192 mM glycine; 0.1% (W/V) SDS) and run at constant voltage (200 V/gel), for 60 minutes. Afterwards, the proteins were transferred for 75 minutes, at 200 V and 110 mA, to a nitrocellulose membrane (Amersham Biosciences) in transfer buffer (pH 8.3: Glycine 192mM, Tris 25mM, methanol 20% v/v) using a semi-dry system (Hoefer SemiPhor Transphor Unit, Amersham Biosciences). To confirm the efficiency of the transference process, the nitrocellulose membrane was counterstained with Ponceau S (Ponceau S 0,5%; TCA 5%). After that, the membrane

was washed in Tris-Buffered saline Tween-20 (TBST- Tris-HCL 20 mM, NaCl 137 mM, 0,1% (v/v) Tween-20) and blocked with 5% milk solution in TBST during 1 hour in slow agitation. After blocking, the membrane was washed in 1% milk solution in TBST during 10 minutes and incubated with primary antibody (*rabbit* anti-cyclin B, 1:4000, Sigma; *mouse* anti-actin, 1:2500, Santa Cruz Biotechnology) diluted in 1% milk solution with PBST, during 1 hour at room temperature. Finally, the membrane was incubated with the secondary antibody linked to HRP (*horseradish peroxidase*) diluted 1:2000, preceded by membrane washing in 1% milk solution with PBST. After three washes in TBST during 10 minutes, the last step was the revelation after incubating the membrane with the ECL solution (Tris HCL 100mM pH 8.5, Coumaric acid 90mM, Luminol 250mM, H2O2 30% (v/v)) for 30 minutes.

The results were scanned using the Gel Doc XR densitometer (Bio-Rad) and analyzed by Quantity One 4.6.1 software (Bio-Rad).

Microscopy, image acquisition and processing

The images from immunofluorescence were obtained using a Spinning-disk confocal microscope:(Axio Observer Z1, Zeiss), equipped with AxioCam MR3 camera. The images were acquired with 63x objective lens with the aid of image acquisition AxioVision 4.8.2, ImageJ version 1.44 (http://rsb.info.nih.gov/ij/) and finally processed using Photoshop CS5 software (Adobe Microsystems, CA).

Results and discussion

1. CDC20 as a potential biomarker for OSCC

In order to analyze CDC20 expression in OSCC tissues, we performed immunohistochemistry assays in formalin-fixed human OSCC and microarrays in paraffin-embedded tissue. The results obtained from these assays were compared to normal tissues in the same conditions.

Using Chi-square test, we analyzed the correlation between CDC20 expression and some of the OSCC clinicopathological features. Using Kaplan-Meier method, we analyzed whether CDC20 expression and other clinicopathological characteristics were correlated with Cancer-Specific Survival (CSS) and Recurrence-Free Survival (RFS).

1.1 Evaluation of CDC20 expression in human OSCC tissues

Immunohistochemistry analysis was carried out in human OSCC tissues using anti-CDC20 monoclonal mouse antibody to evaluate the extent and patterns of CDC20 protein expression. In order to demonstrate the antibody specificity, we used a negative control with PBS instead of antibody, for which no CDC20 staining was observed, as expected.

The expression of CDC20 was observed as nuclear and cytoplasmic staining in both normal and tumor tissues and it was assessed and scored under light microscopy (Figure 1). The intensity of protein expression was not evaluated since it was uniform in most of the tissues. Normal oral mucosa tissue was used as a control, which showed CDC20 staining in its epithelial cells.

CDC20 expression was observed in all OSCC cases, with a mean labeling index of 14.14±10.15 (range 2.4-50.1). The positive CDC20 staining of tumor cells was seen either in a random pattern or with greater distribution at the periphery of the tumor islands, which is considered to be an area of active cell division. As shown in Table 1, out of the 65 cases examined, 37 (56.9%) showed high-level of CDC20 expression, according to the cut-off value of 10%. The other 28 cases (43,1%) were not significantly different from the control.

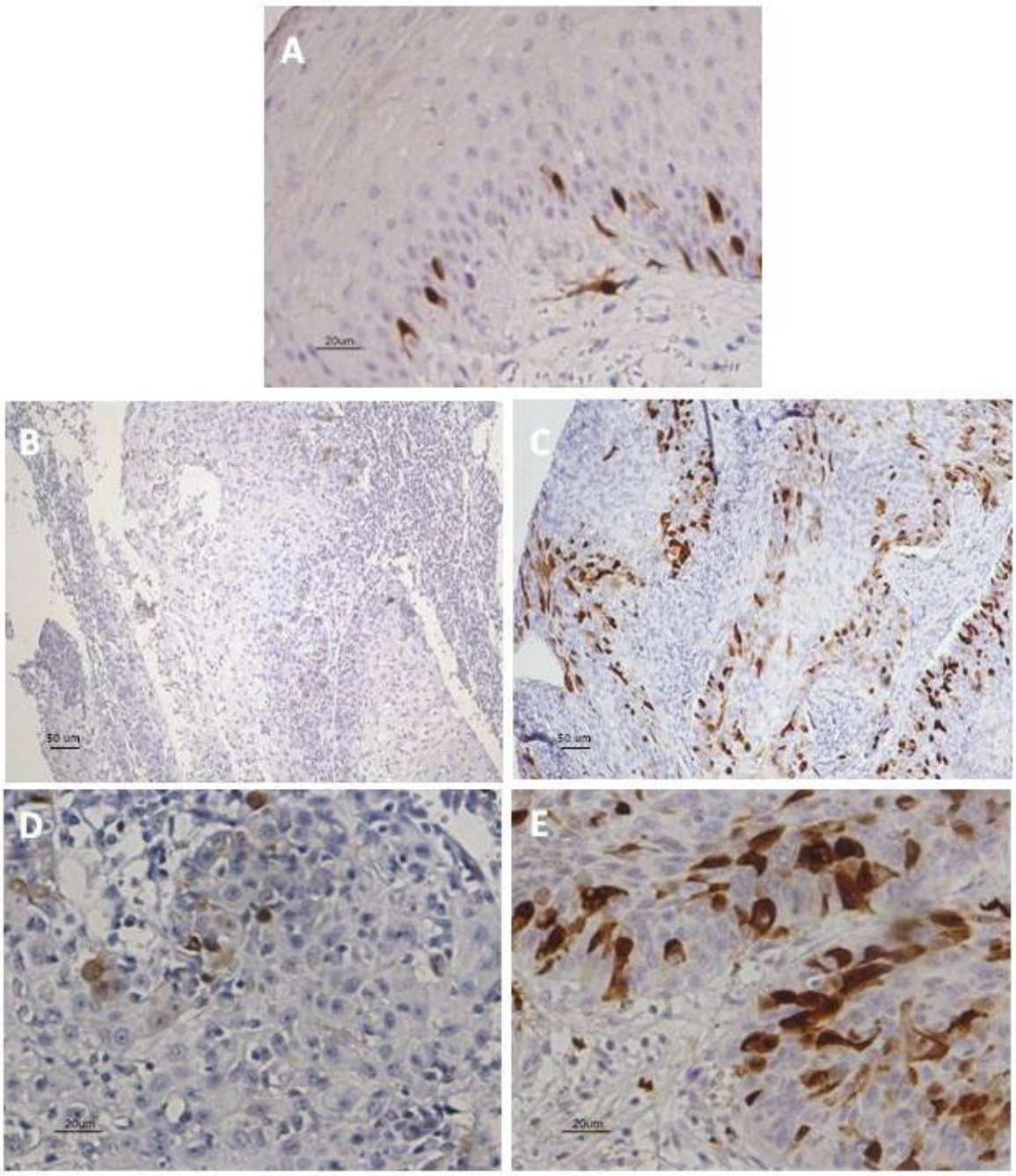

Figure 6: CDC20 protein expression in oral squamous cell carcinoma (OSCC). CDC20 was detected by immunohistochemistry using monoclonal mouse anti-CDC20 antibody; counterstaining was performed with haematoxylin. A: CDC20 staining in epithelial cells in normal oral mucosa, x400. B D: Low levels of CDC20 expression in OSCC, x100 and x400. C E: High levels of CDC20 expression in OSCC, x100 and x400. The scale bar is indicated at the left lower corner of each figure.

1.2 CDC20 expression and its correlation to clinicopathological parameters in OSCC

Having demonstrated that human OSCC tissues expressed high levels of the CDC20 protein, we performed a correlation analysis in an attempt to explore the clinicopathological significance of its expression. Therefore, in OSCC tissue samples, CDC20 protein expression was compared with patient gender and age; tumor location, size, stage, grade, margin, and N status; perineural permeation; and lymphatic invasion (Table 1).

The median age of patients at the time of diagnosis was 61.97 years (range, 25–96 years) and 78.5% of patients were men. Using the Chi-square test, we found no significant association between CDC20 expression and the clinicopathological characteristics listed on Table 1.

Table 1: Association between CDC20 expression and clinicopathological characteristics in patients with oral squamous cell carcinoma

Factor	N (%)	Cdc20		
		Low	High	*p*-value[b]
All cases				
	65 (100%)	28 (43,1%)	37 (56.9%)	
Gender				
Female	14 (21.5%)	7 (50)	7 (50)	0.555
Male	51 (78.5%)	21 (41.2)	30 (58.8)	
Age				
< 62 years	32 (43.8%)	16 (46.9)	17 (53.1)	0.543
≥ 62 years	33 (60.6%)	13 (39.4)	20 (54.1)	
Location				
Floor of the mouth	9 (13.8%)	2 (22.2)	7 (77.8)	
Tongue	21 (32.3%)	9 (42.9)	12 (57.1)	
Buccal mucosa	10 (15.4%)	5 (50)	5 (50)	0.451
Retromolar trigone	10 (15.4%)	4 (40)	6 (60)	
Hard palate	8 (12.3%)	6 (75)	2 (25)	
Gingiva	7 (10.8%)	2 (28.6)	5 (71.4)	
Tumor Size				
T1	9 (13.8%)	5 (55.6)	4 (44.4)	
T2	26 (40.0%)	10 (38.5)	16 (61.5)	0.664
T3	9 (13.8%)	5 (55.6)	4 (44.4)	
T4	21 (32.3%)	8 (38.1)	13 (61.9)	
***N* status**				
N0	35 (53.8%)	15 (42.9)	20 (57.1)	
N1	11 (16.9%)	6 (54.5)	5 (45.4)	0.741
N2	15 (23.1%)	5 (33.3)	10 (66.7)	
N3	4 (6.2%)	2 (50)	2 (50)	
Stage				
I	9 (13.8%)	5 (55.6)	4 (44.4)	
II	20 (30.8%)	8 (40)	12 (60)	0.462
III	10 (15.4%)	6 (60)	4 (40)	
IV	26 (40.0%)	9 (34.6)	17 (65.4)	
Treatment				
SG	26 (40%)	13 (50)	13 (50)	
SG+RT	18 (27.7%)	8 (44.4)	10 (55.6)	0.513
CT+SG or RCT	21 (32.2%)	7 (33.3)	14 (66.7)	
Tumor Grade				
G1	37 (56.9%)	18 (50)	18 (50)	0.151
G2+G3	28 (43.1%)	9 (32.1)	19 (67.9)	
Margin status[a]				
Free of tumor	28 (58.3%)	14 (50)	14 (50)	0.732
With tumor	20 (41.7%)	9 (45)	11 (55)	
Perineural permeation				
absent	58 (89.2%)	27 (46.6)	31 (53.4)	0.103
present	7 (10.8%)	1 (14.3)	6 (85.7)	
Lymphatic invasion				
absent	51 (78.5%)	23 (45.1)	28 (54.9)	0.530
present	14 (21.5%)	5 (35.7)	9 (64.3)	

[a] Not available in the 17 cases.
[b] Chi-square test.

1.3 CDC20 expression and prognostic significance in OSCC

To further understand the clinical significance of CDC20 expression in OSCC, we studied its correlation with Cancer-Specific Survival (CSS) or Recurrence-Free Survival (RFS), in order to verify the potential of CDC20 as a prognostic marker.

By the end of patient follow-up, 33 (50.8%) patients were alive without oral cancer, one patient (1.5%) was alive with oral cancer, and 31 (47.7%) had died as a result of oral cancer. The follow-up mean for all patients was 32.44±26.16 months and the follow-up mean for the surviving patients was 45.87±26.90 months. The cumulative 3-year CSS was 52.3% and RFS was 45%.

The clinicopathological characteristics and CDC20 expression variables were analyzed in univariable analysis using the Kaplan-Meier procedure, a method of estimating time-to-event models in the presence of censored cases, to see their influence on the survival of the patients with OSCC. The unvariable analysis showed that a low CSS (P=0.018) with short median survival periods (40 months) was more significantly associated with high CDC20 protein expression than with low CDC20 expression (68 months) (Figure 7; Table 2). Among the clinicopathological characteristics, tumor size (P<0.001), N status (P=0.003), tumor stage (P<0.001), treatment modality (P<0.001), and histological grade (P=0.020) were statistically associated with a low CSS (Table 2). Additionally, as detailed in table 2, we observed a significant association between RFS and gender (P=0.001), tumor size (P=0.002), N status (P=0.001), tumor stage (P=0.004), and treatment modality (P=0.007).

In order to investigate the independent effects of the variables with significant results in univariable analysis, we included them into multivariable Cox proportional hazards regression model (Tables 3 and 4). We found an independent prognostic value for CDC20 expression where patients with tumors expressing high levels of CDC20 had shown lower CSS than patients with tumors expressing low levels of CDC20 (P=0.032) (Table 3).

We also found an independent prognostic value for tumor size (P = 0.007) correlated with lower CSS (Table 3). Despite CDC20 being correlated with poor prognosis, it is not correlated with RFS (Figure 8). For RFS, we found an independent prognostic value for N status (P = 0.001) and sex (P = 0.001).

Taken together, these results indicate that, besides its previously suggested role in tumorigenesis [90], CDC20 might also be a prognostic marker in oral squamous cell carcinoma. Similarly, CDC20 overexpression has been reported as a poor prognostic

factor in primary non-small cell lung cancer [82] and pancreatic ductal adenocarcinoma [81], indicating that this might be a general feature in human cancers.

Table 2: Univariable analysis of cancer-specific and recurrence-free survival at 3 years, according to clinicopathological characteristics and CDC20 expression in oral squamous cell carcinoma patients

Factor	N	dead	Cancer specific survival[a]	*P*-value[b]	N[c]	recurrence	Recurrence free survival[a]	*P*-value[b]
Gender								
Female	14	8	49	0.228	12	10	25.0	0.001
Male	51	23	53.8		43	18	51.1	
Age								
<62 yrs	32	18	40.7	0.231	25	15	31.5	0.283
≥62 yrs	33	13	63.6		30	13	56.1	
Location								
Floor of the mouth	9	5	66.7		9	7	22.2	
Tongue	21	9	60.3		18	7	64.9	
Buccal mucosa	10	3	65		9	2	66.7	
Retromolar trigone	10	6	28.6	0.129	7	4	35.7	0.108
Hard palate	8	3	60		7	4	42.9	
Gingiva	7	5	28.6		5	4	20	
Tumor size								
T1	9	1	85.7		9	4	62.5	
T2	26	8	70.6	<0.001	26	9	61.9	0.002
T3	9	5	30.5		8	5	30.0	
T4	21	17	19.3		12	10	16.7	
N status								
0	35	10	75.6		32	11	64.2	
1	11	6	19.4	<0.001	10	7	18.0	0.001
2	15	13	10.7		11	9	0	
3	4	2	50		2	1	50.0	
Stage								
I	9	1	85.7		9	4	62.5	
II	20	5	78.9	<0.001	20	6	66.3	0.004
III	10	5	33.3		9	5	34.6	
IV	26	20	21.2		17	13	19.6	
Treatment								
SG	26	4	91.7		26	7	72.7	
SG+RT	18	11	40.0	<0.001	18	13	23.8	0.007
CT+SG or RCT	21	16	18.9		11	8	22.7	
Tumor grade								
G1	37	12	65.8	0.020	32	13	56.6	0.101
G2/G3	28	19	36.8		23	15	30.4	
Margin status[d]								
Free of tumor	28	9	75.7		26	9	61.2	
With tumor	20	10	43.6	0.222	20	13	30.0	0.054
Perineural permeation								
Absent	58	26	55.4	0.126	48	23	47.5	0.110
Present	7	5	28.6		7	5	28.6	
Lymphatic invasion								
Absent	51	25	52.7	0.864	42	23	42.6	0.633
Present	14	6	55.1		13	5	61.5	
CDC20								
Low (0-9%)	28	9	68.0	0.018	25	12	54	0.553
High (10-100%)	37	22	40.2		30	16	37.7	

[a]Percentage of cases without event at 3 years of follow-up (Kaplain Meier estimates of probability of survival).
[b]Log-rank test.
[c] Patients with persistence of the disease were excluded.
[d] Information not available for every patient.

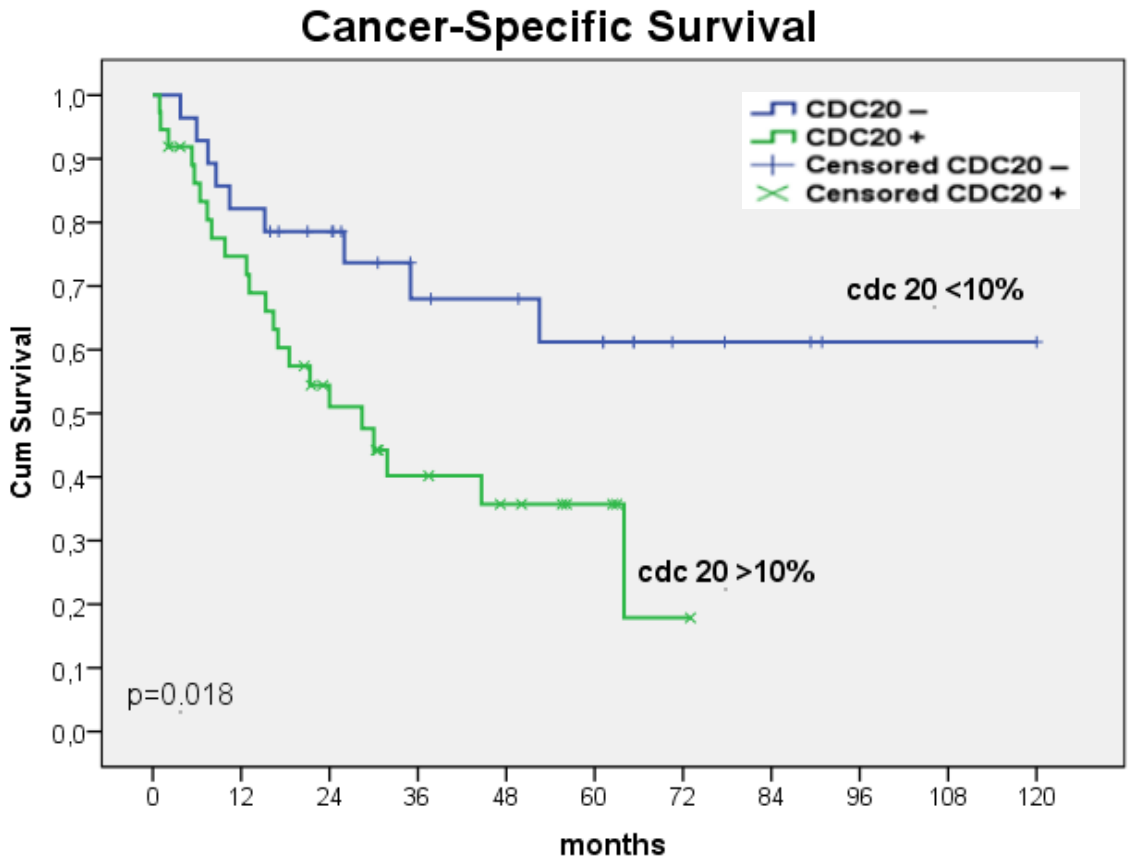

Figure 7: Univariable Kaplan-Meier analysis of cause-specific survival in oral squamous cell carcinoma patients. High CDC20 expression was associated with low overall survival in OSCC patients.

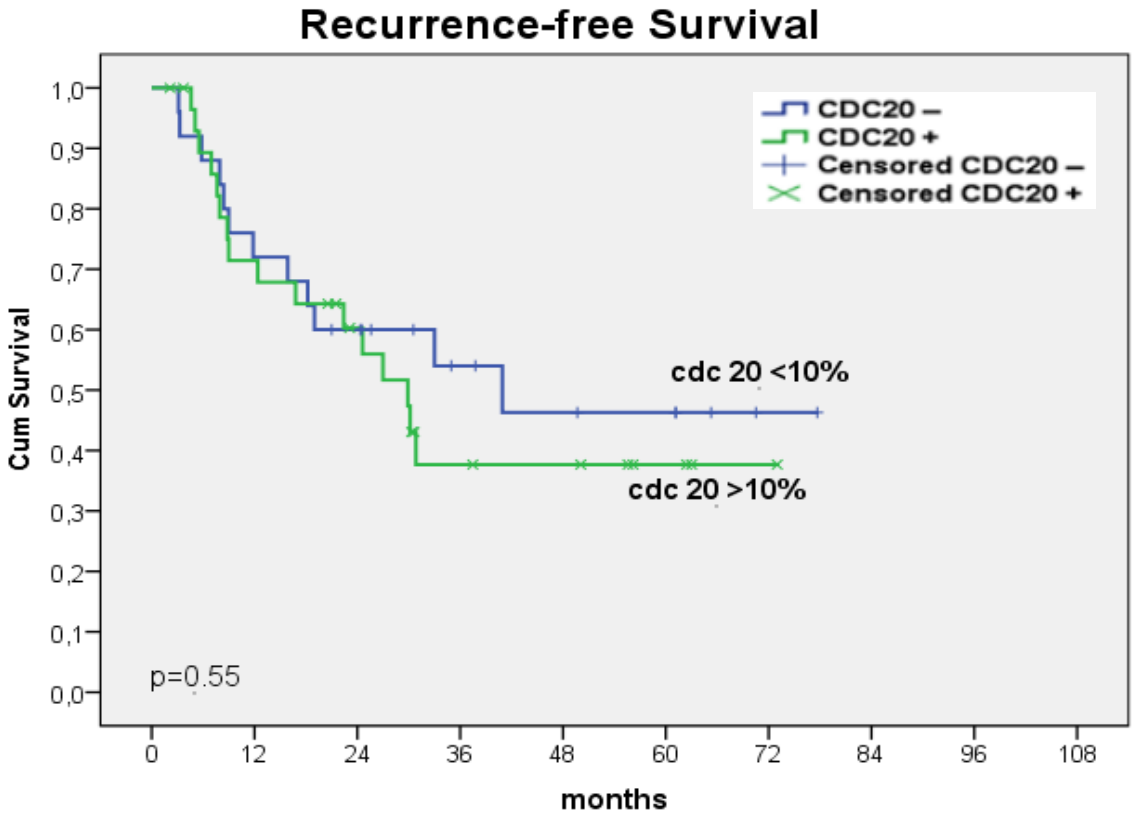

Figure 8: Univariable Kaplan-Meier analysis of cause-specific recurrence-free survival in oral squamous cell carcinoma patients. High CDC20 expression was not associated with recurrence- free survival in OSCC patients. The vertical lines and the "x" signals indicate the censored events.

Table 3: Multivariable analysis of cancer-specific survival on variables with significant independent effect, according to tumor grade, N status, clinical stage, treatment modality, T status and CDC20 expression in oral squamous cell carcinoma patients

Variable[a]	*p-value*	HR	95% CI
Tumor grade[b]	0.843	1.090	0.463-2.567
N status[c]	0.463	0.845	0.538-1.325
Clinical stage[d]	0.273	1.495	0.728-3.070
Treatment modality[e]	0.174	1.467	0.845-2.548
T status[f]	0.000	2.310	1.575-3.387
CDC20 expression[f]	0.032	2.360	1.077-5.170

HR, Hazard ratio; CI, confidence interval for HR.

[a] Variables included in multivariable Cox regression analysis using backward conditional method: T status (ordinal variable); N status (ordinal variable); clinical stage (ordinal variable); treatment modality (ordinal variable); tumor grade, G2+G3 vs G1 (reference category); and CDC20 expression, positive vs negative (reference category). [b] at step 1.[c] at step 2; [d] at step 3; [e] at step 4; [f] at step 5;

Table 4: Multivariable analysis of recurrence-free survival on variables with significant effect, according to T status, clinical stage, N status, treatment modality and gender in oral squamous cell carcinoma patients

Variable[a]	*p-value*	HR	95% CI
T status[b]	0.978	0.989	0.467-2.097
Clinical stage[c]	0.440	1.295	0.672-2.494
N status[d]	0.050	1.548	0.999.2.399
Treatment modality[d]	0.089	1.608	0.930-2.782
Gender[d]	0.000	4.824	2.069-11.245

HR, Hazard ratio; CI, confidence interval for HR.

[a] Variables included in multivariable Cox regression analysis using backward conditional method: gender, female vs male (reference category); T status (ordinal variable); N status (ordinal variable); clinical stage (ordinal variable); and treatment modality (ordinal variable). [b] at step 1.[c] at step 2; [d] at step 3.

2. CDC20 as a potential therapeutic target

Concluded the previous studies from which we can infer that CDC20 might be used as biomarker to predict poor prognosis in OSCC patients, we evaluated its potential as a therapeutic target in the HeLa cancer cell line. For this purpose, the gene encoding the CDC20 protein was silenced by RNA interference and the resultant cell phenotype was analyzed.

2.1 Evaluation of CDC20 protein depletion efficiency

2.1.1 CDC20 depletion in HeLa cell line was effective

Before proceeding to the phenotype analysis, it was necessary to examine the efficiency of CDC20 silencing in HeLa cells.

CDC20 silencing was carried out by siRNA against mRNA encoding the CDC20 protein. We chose the HeLa cell line since it has a good response to RNAi technique.

CDC20 depletion in HeLa cells was evaluated by immunofluorescence with specific anti-CDC20 antibody providing protein detection and localization, 72 hours after transfection. Under fluorescence microscope, we observed in HeLa control cells that CDC20 is localized on kinetochores with bright staining intensity in prometaphase, as show in figure 4, which considerably decreases in metaphase. This result is in agreement with what has been described in the literature [34]. In transfected cells with siRNA oligonucleotides against CDC20, as expected, no protein labeling was not observed (figure 4). This result attests that the siRNA oligonucleotides are efficient in CDC20 silencing.

In addition, using protein extracts isolated from control and transfected cells, western blot technique was performed to indirectly analyze the efficiency of CDC20 protein depletion. Since we didn't achieve any labelling with anti-CDC20 antibody, we used cyclin B as an alternative protein mark. This way, the membrane with the transferred proteins was incubated with the following antibodies: *rabbit* anti-cyclin B (≈ 62 KDa) and *mouse* anti-actin (42 KDa). The actin protein, whose expression is constant among different cell lines, was used as loading control allowing comparison between the bands from the control and transfected cells. Cyclin B, a regulatory protein involved in cell cycle regulation, is required for the activation of mitosis. Its expression increases during prometaphase and metaphase and dramatically decreases in anaphase

due to its degradation by the proteosome. Since CDC20 is required to target cyclin B for proteasomal degradation, its depletion is expected to in an increase in cyclin B expression levels in protein extracts isolated 72h after transfection. However, the results were not conclusive. This is probably due to the fact that anti-cyclin B antibody leads to several unspecific bands, rendering the results interpretation impossible.

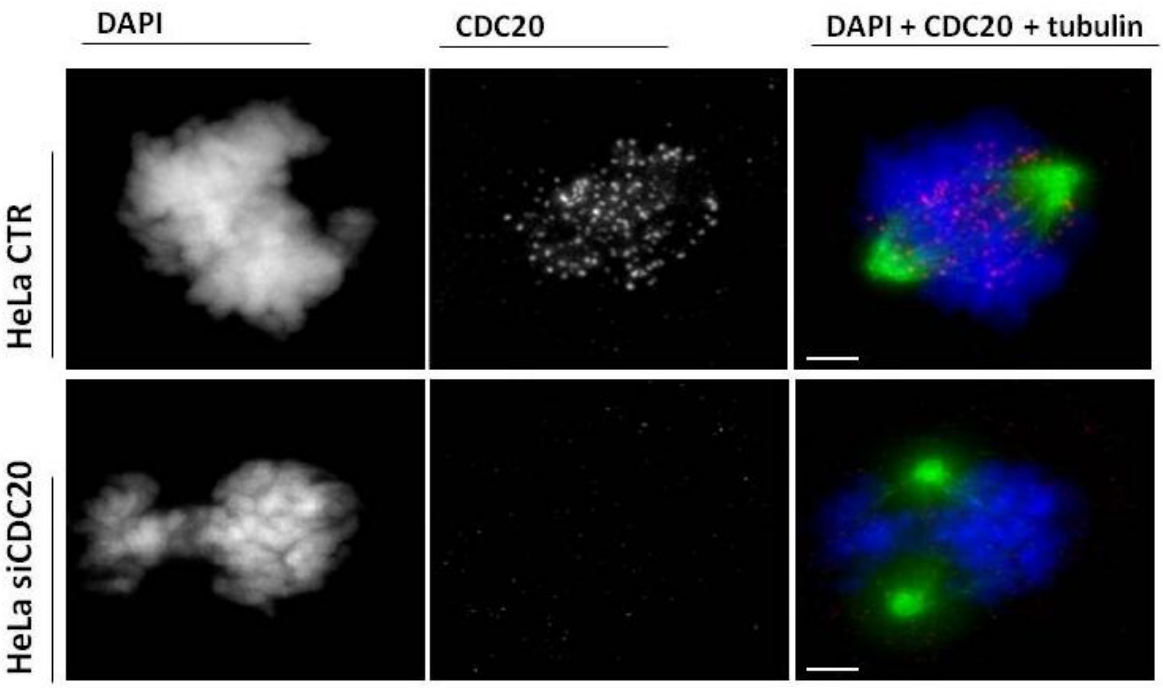

Figure 9: Depletion efficiency of CDC20 protein by RNAi. Images obtained by immunofluorescence of HeLa cells at prometaphase with anti-CDC20 (red) and anti-α-tubulin (Green) staining; The DNA (blue) was stained with DAPI. In the control situation (CTR) there is a strong staining of CDC20 in kinetochores that is undetectable in cells after CDC20 depletion (siCDC20). Bar = 5µm.

2.2 Analysis of the phenotype resulting from CDC20 depletion

2.2.1 CDC20 depletion causes mitotic arrest and cell death

After ensuring the effectiveness of CDC20 silencing, the resultant phenotype was analyzed.

We observed that silencing of CDC20 gene by RNAi induced cell arrest in mitosis. Under phase contrast microscope visualization, mitotic cells can be distinguished by being brighter with a round shape, while the interphasic cells have a slightly elongated shape. As show in figure 10, a high number of cells are arrested in mitosis comparatively to control cells, 72h after transfection, using the phase contrast microscope. This result was also confirmed after cytospin and DNA staining with DAPI as show in figure 11, where we can see that the rounded cells were indeed cells arrested in mitosis, with condensed chromosomes (indicated by an arrow). This result is in line with some research works that similarly reported that CDC20 knockdown leads to mitotic arrest [95-97].

As it was shown that cells are arrested in mitosis after 72h of CDC20 depletion, cells were submitted to 96h of transfection to see the resulting effect: whether they undergo cell death or continue the cell cycle division. As shown in figure 10, in transfected cells, we can see dead cells in suspension. Additionally, in figure 11 we can see micro-nucleus indicating cell death.

Nevertheless, the role of CDC20 in human cell cycle is controversial. There are some research works showing that the interference with CDC20 is compatible with cell viability in a functional spindle checkpoint [98, 99]. Malureanu *et al.* constructed hypomorphic mice expressing small amounts of CDC20 and showed that these mice were healthy but with substantial aneuploidy [100]. Another study, using an inducible lentiviral short-hairpin (sh) RNA system, demonstrated that cells were not blocked in mitosis [101].

The present results support that blocking CDC20 results in mitotic arrest. The differences between this study and the previous ones may be explained by the different levels of CDC20 depletion efficiency which were obtained in their results, since it may affect the way in which the cells are arrested in mitosis.

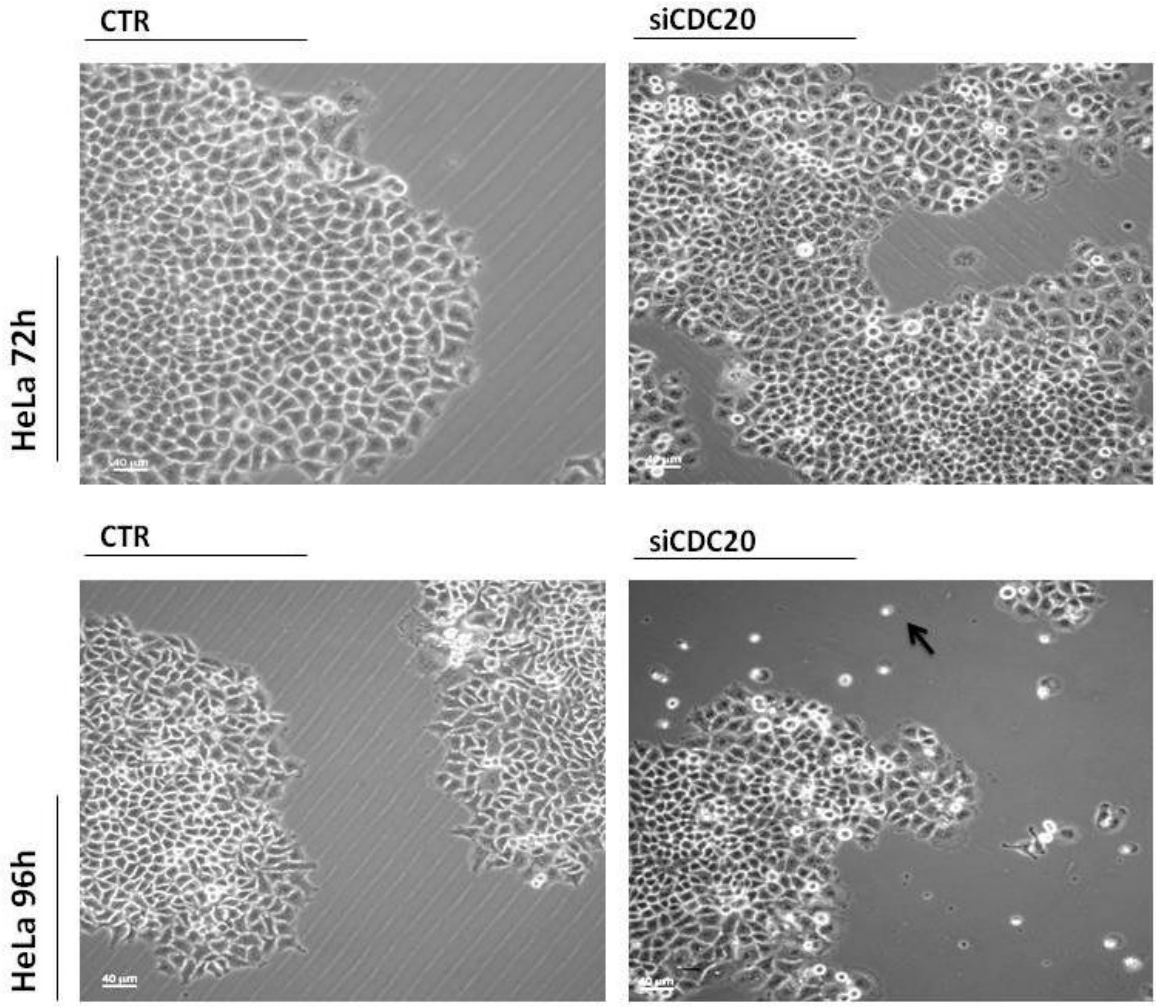

Figure 10: Depletion of CDC20 protein induces an accumulation of cells in mitosis and cell death. Images obtained by phase contrast microscopy of HeLa cells in culture. 72 hours after CDC20 depletion (siCDC20), an increase in mitotic cells (round configuration) is visible comparatively to the control situation (CTR). 96 hours after CDC20 depletion, the mitotic cells seem to undergo cell death (black arrow), a phenotype non-observable in the control situation. Bar = 40 µm.

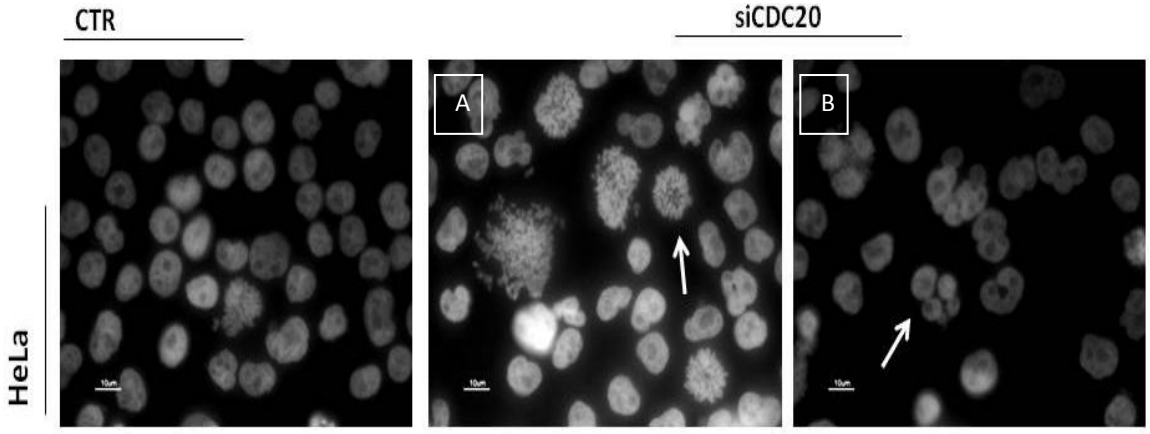

Figure 11: Depletion of CDC20 protein induces an accumulation of cells in mitosis and cell death. Fluorescence microscope images from cytospin 72 hours after depletion of CDC20. A: transfected cells show an increase of cells arrested in mitosis with condensed chromosomes (white arrow) compared to the control situation. B: presence of micro-nucleus (white arrow) indicating cell death after depletion of CDC20. Bar = 10 µm.

Besides cell cycle arrest in mitosis, we observed micro-nucleus formation in the transfected cells, suggesting that these cells undergo cell death. These assays were also performed in the SCC25 cell line. However, the phenotype analysis was inconclusive because, despite the transfection efficiency, the resultant phenotype did not show significant changes.

Current anti-mitotic drugs that target microtubule dynamics, such as taxanes and vinca alkaloids, cause mitotic arrest by activating SAC and, consequently, kill cells by triggering apoptosis [5, 21]. However, many cancer cells can exit mitosis prematurely due to a weak SAC activity that does not fully respond to mitotic errors, thereby resisting such killing [71, 72]. It was shown that, independently of SAC activity, RNAi-mediated knockdown of CDC20 slowed cyclin B1 degradation, giving more time to cancer cells to initiate cell death [96]. Our results fundament this idea, since we demonstrated that CDC20 depletion leads to mitotic arrest, and consequently, to cell death. Taken together, these results lead to the conclusion that targeting CDC20-mediated mitotic exit is a better therapeutic approach than perturbing spindle assembly.

Conclusion

Conclusion

The spindle assembly checkpoint (SAC) is a crucial surveillance mechanism that ensure accurate sister chromatid segregation avoiding genetic instability [3, 40]. CDC20, as a core SAC protein, has been found in several cancers type, including oral squamous cell carcinoma, with high expression levels [90]. In this line, with this project we aimed to study the clinic significance of CDC20 in tissues from OSCC patients evaluating its expression and their association with clinicopathological characteristics and patient survival, in order to evaluate it as a prognostic biomarker and as a potential therapeutic target.

Our results reveal that: **(1)** CDC20 shows high expression levels in human OSCC tissues than in normal oral mucosa tissues; **(2)** An independent prognostic value was found for CDC20 where tumors with high expression of CDC20 had lower Cancer-Specific Survival (CSS) comparatively to those with low expression levels; **(3)** Depletion of CDC20 by interference RNA assay causes mitotic arrest and cell death in HeLa cell line.

In conclusion, our results identify high CDC20 expression as an independent prognostic marker of overall cancer-specific survival in patients with OSCC. Given the poor prognosis of such tumor and lack of therapeutic options available to them, clearly shows the importance of this study where high CDC20 expression could serve as a molecular marker to identify high-risk subgroups for OSCC therapy.

Moreover, ours results in HeLa cell line by interference RNA have also demonstrated that CDC20 is an essential protein for mitosis and cell survival and could be useful in anti-cancer therapy.

Future prospects

Future prospects

The obtained results lead to some expectations and new research routes to explore. After finding the role of CDC20 as a biomarker in OSCC, further investigations are needed to complement the results here obtained and, in this way, bring us closer to the clinical use of this protein's predictive potential.

In this work, HeLa cells were used since they are a standard cell line used for cancer studies. Its cellular pathways are well known and characterized and it grows in common laboratory conditions, making it an easy cell line to work with and obtain preliminary results. However, it is essential to confirm our findings in an OSCC cell line. We attempted to use the SCC25 cell line but the results were inconclusive. These assays need, therefore, to be repeated, using a normal oral cavity cell line as a control. Only then can these observations be transposed to OSCC. In addition, regarding the cell death observed in the phenotype resultant from transfected cells, the next step would be the performance of cell death evaluation assays such as trypan blue exclusion and LDH cytotoxicity detection.

In a long term perspective, it is also possible to design an *in vivo* study, for instance, inducing cancer in mice using xenografts and analyzing the reaction to treatment with siRNA CDC20.

After following these steps, it will be possible to known with more certainty whether CDC20 can be used as a therapeutic target in OSCC. In affirmative case, one viable option would be nanoencapsulation of the siRNA oligonucleotides against CDC20.

References

References

1. Juliana Faria, J.B., Inês M. B. Moura, Rui M. Reis, Hassan Bousbaa, *The Spindle Assembly Checkpoint and Aneuploidy*, in *Aneuploidy: Etiology, Disorders and Risk Factors*. 2012. p. 59-75.
2. Hausman, G.M.C.a.R.E., *The Cell A Molecular Approach*. 2007.
3. Musacchio, A. and E.D. Salmon, *The spindle-assembly checkpoint in space and time.* Nat Rev Mol Cell Biol, 2007. **8**(5): p. 379-93.
4. Abrous, D.N., M. Koehl, and M. Le Moal, *Adult neurogenesis: from precursors to network and physiology.* Physiol Rev, 2005. **85**(2): p. 523-69.
5. Manchado, E., M. Guillamot, and M. Malumbres, *Killing cells by targeting mitosis.* Cell Death Differ, 2012. **19**(3): p. 369-77.
6. Kaestner, P., A. Aigner, and H. Bastians, *Therapeutic targeting of the mitotic spindle checkpoint through nanoparticle-mediated siRNA delivery inhibits tumor growth in vivo.* Cancer Lett, 2011. **304**(2): p. 128-36.
7. He, E., et al., *System-level feedbacks make the anaphase switch irreversible.* Proc Natl Acad Sci U S A, 2011. **108**(24): p. 10016-21.
8. Schafer, K.A., *The cell cycle: a review.* Vet Pathol, 1998. **35**(6): p. 461-78.
9. Bruce Alberts, A.J., Julian Lewis, Martin Raff, Keith Roberts, and Peter Walter., *Molecular Biology Of The Cell*. 2002.
10. DeWolf, W.C. and S.M. Gaston, *The cell cycle and its relevance to the urologist.* J Urol, 2004. **171**(4): p. 1674-81.
11. Brooks, G. and N.B. La Thangue, *The cell cycle and drug discovery: the promise and the hope.* Drug Discov Today, 1999. **4**(10): p. 455-464.
12. Harvey Lodish, A.B., Paul Matsudaira, Chris A. Kaiser, Monty Krieger, Matthew P. Scott, Lawrence Zipursky, James Darnell, *Molecular Cell Biology*. 2000.
13. Doree, M. and T. Hunt, *From Cdc2 to Cdk1: when did the cell cycle kinase join its cyclin partner?* J Cell Sci, 2002. **115**(Pt 12): p. 2461-4.
14. Tyson, J.J., A. Csikasz-Nagy, and B. Novak, *The dynamics of cell cycle regulation.* Bioessays, 2002. **24**(12): p. 1095-109.
15. Michalides, R.J., *Cell cycle regulators: mechanisms and their role in aetiology, prognosis, and treatment of cancer.* J Clin Pathol, 1999. **52**(8): p. 555-68.
16. Nigg, E.A., *Mitotic kinases as regulators of cell division and its checkpoints.* Nat Rev Mol Cell Biol, 2001. **2**(1): p. 21-32.
17. Kops, G.J., B.A. Weaver, and D.W. Cleveland, *On the road to cancer: aneuploidy and the mitotic checkpoint.* Nat Rev Cancer, 2005. **5**(10): p. 773-85.
18. Lebedeva, L.I., et al., *[Mitosis: regulation and organization of cell division].* Genetika, 2004. **40**(12): p. 1589-608.
19. Doxsey, S., W. Zimmerman, and K. Mikule, *Centrosome control of the cell cycle.* Trends Cell Biol, 2005. **15**(6): p. 303-11.
20. O'Connell, C.B., A. Khodjakov, and B.F. McEwen, *Kinetochore flexibility: creating a dynamic chromosome-spindle interface.* Curr Opin Cell Biol, 2012. **24**(1): p. 40-7.
21. Zhou, J. and P. Giannakakou, *Targeting microtubules for cancer chemotherapy.* Curr Med Chem Anticancer Agents, 2005. **5**(1): p. 65-71.
22. Cheeseman, I.M. and A. Desai, *Molecular architecture of the kinetochore-microtubule interface.* Nat Rev Mol Cell Biol, 2008. **9**(1): p. 33-46.
23. Maiato, H., et al., *The dynamic kinetochore-microtubule interface.* J Cell Sci, 2004. **117**(Pt 23): p. 5461-77.
24. Zhou, J., J. Yao, and H.C. Joshi, *Attachment and tension in the spindle assembly checkpoint.* J Cell Sci, 2002. **115**(Pt 18): p. 3547-55.

25. Vermeulen, K., D.R. Van Bockstaele, and Z.N. Berneman, *The cell cycle: a review of regulation, deregulation and therapeutic targets in cancer.* Cell Prolif, 2003. **36**(3): p. 131-49.
26. Murray, A.W., *Recycling the cell cycle: cyclins revisited.* Cell, 2004. **116**(2): p. 221-34.
27. Sullivan, M. and D.O. Morgan, *Finishing mitosis, one step at a time.* Nat Rev Mol Cell Biol, 2007. **8**(11): p. 894-903.
28. Abraham, R.T., *Cell cycle checkpoint signaling through the ATM and ATR kinases.* Genes Dev, 2001. **15**(17): p. 2177-96.
29. Sherr, C.J. and J.M. Roberts, *Living with or without cyclins and cyclin-dependent kinases.* Genes Dev, 2004. **18**(22): p. 2699-711.
30. Gong, H., *[Advance of study on effects of Chfr gene of mitosis prophase checkpoint--review].* Zhongguo Shi Yan Xue Ye Xue Za Zhi, 2004. **12**(6): p. 870-4.
31. Kang, D., et al., *The checkpoint protein Chfr is a ligase that ubiquitinates Plk1 and inhibits Cdc2 at the G2 to M transition.* J Cell Biol, 2002. **156**(2): p. 249-59.
32. Hardwick, K.G. and J.V. Shah, *Spindle checkpoint silencing: ensuring rapid and concerted anaphase onset.* F1000 Biol Rep, 2010. **2**: p. 55.
33. Bharadwaj, R. and H. Yu, *The spindle checkpoint, aneuploidy, and cancer.* Oncogene, 2004. **23**(11): p. 2016-27.
34. Logarinho, E., et al., *The human spindle assembly checkpoint protein Bub3 is required for the establishment of efficient kinetochore-microtubule attachments.* Mol Biol Cell, 2008. **19**(4): p. 1798-813.
35. Logarinho, E. and H. Bousbaa, *Kinetochore-microtubule interactions "in check" by Bub1, Bub3 and BubR1: The dual task of attaching and signalling.* Cell Cycle, 2008. **7**(12): p. 1763-8.
36. Sudakin, V., G.K. Chan, and T.J. Yen, *Checkpoint inhibition of the APC/C in HeLa cells is mediated by a complex of BUBR1, BUB3, CDC20, and MAD2.* J Cell Biol, 2001. **154**(5): p. 925-36.
37. Chin, C.F. and F.M. Yeong, *Safeguarding entry into mitosis: the antephase checkpoint.* Mol Cell Biol, 2010. **30**(1): p. 22-32.
38. Silva, P., et al., *Monitoring the fidelity of mitotic chromosome segregation by the spindle assembly checkpoint.* Cell Prolif, 2011. **44**(5): p. 391-400.
39. Vogt, E., et al., *Spindle formation, chromosome segregation and the spindle checkpoint in mammalian oocytes and susceptibility to meiotic error.* Mutat Res, 2008. **651**(1-2): p. 14-29.
40. May, K.M. and K.G. Hardwick, *The spindle checkpoint.* J Cell Sci, 2006. **119**(Pt 20): p. 4139-42.
41. Marangos, P. and J. Carroll, *Securin regulates entry into M-phase by modulating the stability of cyclin B.* Nat Cell Biol, 2008. **10**(4): p. 445-51.
42. Nasmyth, K., *How do so few control so many?* Cell, 2005. **120**(6): p. 739-46.
43. Kim, S. and H. Yu, *Mutual regulation between the spindle checkpoint and APC/C.* Semin Cell Dev Biol, 2011. **22**(6): p. 551-8.
44. Suijkerbuijk, S.J. and G.J. Kops, *Preventing aneuploidy: the contribution of mitotic checkpoint proteins.* Biochim Biophys Acta, 2008. **1786**(1): p. 24-31.
45. Holland, A.J. and D.W. Cleveland, *Boveri revisited: chromosomal instability, aneuploidy and tumorigenesis.* Nat Rev Mol Cell Biol, 2009. **10**(7): p. 478-87.
46. Schvartzman, J.M., R. Sotillo, and R. Benezra, *Mitotic chromosomal instability and cancer: mouse modelling of the human disease.* Nat Rev Cancer, 2010. **10**(2): p. 102-15.
47. Fang, X. and P. Zhang, *Aneuploidy and tumorigenesis.* Semin Cell Dev Biol, 2011. **22**(6): p. 595-601.
48. Chi, Y.H. and K.T. Jeang, *Aneuploidy and cancer.* J Cell Biochem, 2007. **102**(3): p. 531-8.

49. Schmidt, M. and R.H. Medema, *Exploiting the compromised spindle assembly checkpoint function of tumor cells: dawn on the horizon?* Cell Cycle, 2006. **5**(2): p. 159-63.
50. Cahill, D.P., et al., *Characterization of MAD2B and other mitotic spindle checkpoint genes.* Genomics, 1999. **58**(2): p. 181-7.
51. Ohshima, K., et al., *Mutation analysis of mitotic checkpoint genes (hBUB1 and hBUBR1) and microsatellite instability in adult T-cell leukemia/lymphoma.* Cancer Lett, 2000. **158**(2): p. 141-50.
52. Kim, H.S., et al., *Frequent mutations of human Mad2, but not Bub1, in gastric cancers cause defective mitotic spindle checkpoint.* Mutat Res, 2005. **578**(1-2): p. 187-201.
53. Tsukasaki, K., et al., *Mutations in the mitotic check point gene, MAD1L1, in human cancers.* Oncogene, 2001. **20**(25): p. 3301-5.
54. Gemma, A., et al., *Somatic mutation of the hBUB1 mitotic checkpoint gene in primary lung cancer.* Genes Chromosomes Cancer, 2000. **29**(3): p. 213-8.
55. Thompson, S.L., S.F. Bakhoum, and D.A. Compton, *Mechanisms of chromosomal instability.* Curr Biol, 2010. **20**(6): p. R285-95.
56. Thoma, C.R., et al., *Mechanisms of aneuploidy and its suppression by tumour suppressor proteins.* Swiss Med Wkly, 2011. **141**: p. w13170.
57. Kops, G.J., D.R. Foltz, and D.W. Cleveland, *Lethality to human cancer cells through massive chromosome loss by inhibition of the mitotic checkpoint.* Proc Natl Acad Sci U S A, 2004. **101**(23): p. 8699-704.
58. Baker, D.J., et al., *BubR1 insufficiency causes early onset of aging-associated phenotypes and infertility in mice.* Nat Genet, 2004. **36**(7): p. 744-9.
59. Dai, W., et al., *Slippage of mitotic arrest and enhanced tumor development in mice with BubR1 haploinsufficiency.* Cancer Res, 2004. **64**(2): p. 440-5.
60. Liu, A.W., et al., *The clinicopathological significance of BUBR1 overexpression in hepatocellular carcinoma.* J Clin Pathol, 2009. **62**(11): p. 1003-8.
61. Hsieh, P.C., et al., *Expression of BUBR1 in human oral potentially malignant disorders and squamous cell carcinoma.* Oral Surg Oral Med Oral Pathol Oral Radiol Endod, 2010. **109**(2): p. 257-67.
62. Jeong, S.J., et al., *Transcriptional abnormality of the hsMAD2 mitotic checkpoint gene is a potential link to hepatocellular carcinogenesis.* Cancer Res, 2004. **64**(23): p. 8666-73.
63. Michel, L., et al., *Complete loss of the tumor suppressor MAD2 causes premature cyclin B degradation and mitotic failure in human somatic cells.* Proc Natl Acad Sci U S A, 2004. **101**(13): p. 4459-64.
64. Wang, L., et al., *Depression of MAD2 inhibits apoptosis and increases proliferation and multidrug resistance in gastric cancer cells by regulating the activation of phosphorylated survivin.* Tumour Biol, 2010. **31**(3): p. 225-32.
65. Hernando, E., et al., *Rb inactivation promotes genomic instability by uncoupling cell cycle progression from mitotic control.* Nature, 2004. **430**(7001): p. 797-802.
66. Sotillo, R., et al., *Mad2 overexpression promotes aneuploidy and tumorigenesis in mice.* Cancer Cell, 2007. **11**(1): p. 9-23.
67. Grabsch, H., et al., *Overexpression of the mitotic checkpoint genes BUB1, BUBR1, and BUB3 in gastric cancer--association with tumour cell proliferation.* J Pathol, 2003. **200**(1): p. 16-22.
68. Ryan, S.D., et al., *Up-regulation of the mitotic checkpoint component Mad1 causes chromosomal instability and resistance to microtubule poisons.* Proc Natl Acad Sci U S A, 2012. **109**(33): p. E2205-14.
69. Fojo, T. and M. Menefee, *Mechanisms of multidrug resistance: the potential role of microtubule-stabilizing agents.* Ann Oncol, 2007. **18 Suppl 5**: p. v3-8.
70. Chan, K.S., C.G. Koh, and H.Y. Li, *Mitosis-targeted anti-cancer therapies: where they stand.* Cell Death Dis, 2012. **3**: p. e411.

71. Schmidt, M. and H. Bastians, *Mitotic drug targets and the development of novel anti-mitotic anticancer drugs.* Drug Resist Updat, 2007. **10**(4-5): p. 162-81.
72. Bolanos-Garcia, V.M., *Assessment of the mitotic spindle assembly checkpoint (SAC) as the target of anticancer therapies.* Curr Cancer Drug Targets, 2009. **9**(2): p. 131-41.
73. Kaestner, P. and H. Bastians, *Mitotic drug targets.* J Cell Biochem, 2010. **111**(2): p. 258-65.
74. Henderson, M.C., et al., *UA62784, a novel inhibitor of centromere protein E kinesin-like protein.* Mol Cancer Ther, 2009. **8**(1): p. 36-44.
75. Bhatt, A.N., et al., *Cancer biomarkers - current perspectives.* Indian J Med Res, 2010. **132**: p. 129-49.
76. Ando, K., et al., *High expression of BUBR1 is one of the factors for inducing DNA aneuploidy and progression in gastric cancer.* Cancer Sci, 2010. **101**(3): p. 639-45.
77. Kato, T., et al., *Overexpression of MAD2 predicts clinical outcome in primary lung cancer patients.* Lung Cancer, 2011. **74**(1): p. 124-31.
78. Chen, Y.J., et al., *Overexpression of Aurora B is associated with poor prognosis in epithelial ovarian cancer patients.* Virchows Arch, 2009. **455**(5): p. 431-40.
79. Takeshita, M., et al., *Aurora-B overexpression is correlated with aneuploidy and poor prognosis in non-small cell lung cancer.* Lung Cancer, 2013. **80**(1): p. 85-90.
80. Lin, Z.Z., et al., *Significance of Aurora B overexpression in hepatocellular carcinoma. Aurora B Overexpression in HCC.* BMC Cancer, 2010. **10**: p. 461.
81. Chang, D.Z., et al., *Increased CDC20 expression is associated with pancreatic ductal adenocarcinoma differentiation and progression.* J Hematol Oncol, 2012. **5**: p. 15.
82. Kato, T., et al., *Overexpression of CDC20 predicts poor prognosis in primary non-small cell lung cancer patients.* J Surg Oncol, 2012. **106**(4): p. 423-30.
83. Tanaka, T. and M. Tanaka, *Oral carcinogenesis and oral cancer chemoprevention: a review.* Patholog Res Int, 2011. **2011**: p. 431246.
84. Guerrero-Preston, R., et al., *NID2 and HOXA9 promoter hypermethylation as biomarkers for prevention and early detection in oral cavity squamous cell carcinoma tissues and saliva.* Cancer Prev Res (Phila), 2011. **4**(7): p. 1061-72.
85. Liviu Feller, J.L., *Oral Squamous Cell Carcinoma: Epidemiology, Clinical Presentation and Treatment* Journal of Cancer Therapy, 2012.
86. Deshpande, A.M. and D.T. Wong, *Molecular mechanisms of head and neck cancer.* Expert Rev Anticancer Ther, 2008. **8**(5): p. 799-809.
87. Bhandary, S. and P. Bhandary, *Cancer of the oral cavity- a growing concern in the Micronesia: a case report from the Marshall Islands.* Pac Health Dialog, 2003. **10**(1): p. 76-8.
88. Minhas, K.M., et al., *Spindle assembly checkpoint defects and chromosomal instability in head and neck squamous cell carcinoma.* Int J Cancer, 2003. **107**(1): p. 46-52.
89. Rizzardi, C., et al., *BUBR1 expression in oral squamous cell carcinoma and its relationship to tumor stage and survival.* Head Neck, 2011. **33**(5): p. 727-33.
90. Mondal, G., et al., *Overexpression of Cdc20 leads to impairment of the spindle assembly checkpoint and aneuploidization in oral cancer.* Carcinogenesis, 2007. **28**(1): p. 81-92.
91. Nilsson, J., *Cdc20 control of cell fate during prolonged mitotic arrest: do Cdc20 protein levels affect cell fate in response to antimitotic compounds?* Bioessays, 2011. **33**(12): p. 903-9.
92. Kim, J.M., et al., *Identification of gastric cancer-related genes using a cDNA microarray containing novel expressed sequence tags expressed in gastric cancer cells.* Clin Cancer Res, 2005. **11**(2 Pt 1): p. 473-82.
93. Singhal, S., et al., *Alterations in cell cycle genes in early stage lung adenocarcinoma identified by expression profiling.* Cancer Biol Ther, 2003. **2**(3): p. 291-8.

94. Marucci, G., et al., *Gene expression profiling in glioblastoma and immunohistochemical evaluation of IGFBP-2 and CDC20.* Virchows Arch, 2008. **453**(6): p. 599-609.
95. Kidokoro, T., et al., *CDC20, a potential cancer therapeutic target, is negatively regulated by p53.* Oncogene, 2008. **27**(11): p. 1562-71.
96. Huang, H.C., et al., *Evidence that mitotic exit is a better cancer therapeutic target than spindle assembly.* Cancer Cell, 2009. **16**(4): p. 347-58.
97. Nilsson, J., et al., *The APC/C maintains the spindle assembly checkpoint by targeting Cdc20 for destruction.* Nat Cell Biol, 2008. **10**(12): p. 1411-20.
98. Clarke, D.J., L.A. Diaz-Martinez, and J.F. Gimenez-Abian, *Anaphase promoting complex or cyclosome?* Cell Cycle, 2005. **4**(11): p. 1585-92.
99. Brummelkamp, T.R., R. Bernards, and R. Agami, *A system for stable expression of short interfering RNAs in mammalian cells.* Science, 2002. **296**(5567): p. 550-3.
100. Malureanu, L., et al., *Cdc20 hypomorphic mice fail to counteract de novo synthesis of cyclin B1 in mitosis.* J Cell Biol, 2010. **191**(2): p. 313-29.
101. Baumgarten, A.J., J. Felthaus, and R. Wasch, *Strong inducible knockdown of APC/CCdc20 does not cause mitotic arrest in human somatic cells.* Cell Cycle, 2009. **8**(4): p. 643-6.